UNIVERSITY OF TURIN

Department of Veterinary Sciences

Doctoral School in Life and Health Sciences

Research Doctorate in Veterinary Sciences for Animal Health and Food Safety

XXXII CYCLE

PhD Thesis

Canine Effusions: an Advanced Clinicopathological Multimodal Approach

PhD Candidate

Maverick Melega

Tutor: Prof. Fulvio Riondato

PhD Coordinator: Prof. Mario Baratta

Academic years 2016-2019

VET/08

TABLE OF CONTENTS

INTRODUCTION **1**
Body Cavities **1**
Pathophysiology of Effusions **2**
Clinicopathological Classification of Effusions **3**
Standard Analysis **5**
Ancillary tests **8**
Non-Hematopoietic Cells in Effusions **10**

AIM **13**

STUDY 1: CELL BLOCKS **14**
1.1 Introduction **14**
1.2 Materials and Methods **14**
1.3 Results **17**
1.4 Discussion and Conclusion **26**

STUDY 2: ADVIA 120 CYTOGRAMS **29**
1.1 Introduction **29**
1.2 Materials and Methods **29**
1.3 Results **32**
1.4 Discussion and Conclusion **36**

STUDY 3: FLOW CYTOEMTRY **39**
1.1 Introduction **39**
1.2 Materials and Methods **39**
1.3 Results **44**
1.4 Discussion and Conclusion **54**

FINAL CONSIDERATIONS **62**

REFERENCES **64**

INTRODUCTION

BODY CAVITIES

Body cavities are virtual spaces that accommodate viscera. Three main cavities are identified in mammalians, the pleural, the pericardial and the peritoneal. In males, the scrotum sac represents an additional cavity which is anatomically and functionally an extension of the peritoneal one, and therefore considered as part of it. Body cavities are covered by a monolayer of mesothelial cells which are the main component of the parietal serosa. Similarly, all viscera are covered by a visceral serosa which has identical features of the parietal one. The primary function of the two serosae is to provide a non-adhesive, frictionless, and protective barrier that facilitates the movements of opposing tissues and organs within the cavities. Additionally, in thorax, these surfaces provide mechanical coupling between the chest wall and the lungs allowing the direct transmission of forces during respiration. Specialized portions of the serosae become supporting and anchoring structures for organs (mesenteries and omentum) and embrace blood and lymphatic vessels.

Serosal surfaces are composed of a monolayer of mesothelial cells laying on a basement membrane supported by submesothelium. Mesothelial cells are mainly elongated, flattened with a squamous appearance. A cuboid variant has been observed near parenchymal organs and within injured or stimulated mesothelium. Although these two types of mesothelial cells have subtle ultrastructural differences, no phenotypical differences were observed (Mutsaers 2004). The luminal surface has numerous microvilli which entrap the fluid and protect the surface from friction, they also increase the area enhancing the efficiency of solute exchange. Additionally, mesothelial cells present cilia. Their function has not been clarified yet; a possible role in the regulation of the synthesis of matrix proteins has been hypothesized. Also, cilia are lacking in proliferating cells while increase with increasing cell density which suggests they play a role in cell polarity and adhesion. (Bird 2004)

During physiological conditions, mesothelial cells present minimal proliferative activity. However, the mitotic rate can increase steeply when they are exposed to any sort injury or stimuli. Morphological changes include enlargement, transformation from squamous to cuboidal or columnar, increase in the N:C ratio, vacuolation, and loss of microvilli (Di Paolo 1986; Williams 2003) and cilia. In presence of a persistent abnormal amount of fluid in the cavity cell-matrix and cell-cell interactions are lost resulting in shedding of mesothelial cells in the fluid (Whitaker and Papadimitrou, 1985). The release of mesothelial cells in the cavity is also induced by direct mechanical injury to the mesothelium; cells exfoliate from other sites in order to attach and incorporate into the damaged mesothelium. (Mutsaers 2000; Comer 2002; Mutsaers, 2004).

Mesothelial cells function is not limited to maintain the fluid homeostasis, they also contribute to fluid and cell movement through the surface, inflammation, tissue repair, prevention of adhesion formation,

and defence. They are directly part of the local immunity system being both phagocytic (Yao 2003) and antigen presenting cells (Mutsaers 2004). They produce a plethora of cytokines, vasoactive mediators and immunomodulators able to recruit monocyte and neutrophils from the blood, initiate, maintain, and terminate the inflammatory response (Jantz 2008). Finally, they produce fibrinolytic molecules to prevent fibrous adhesions in post inflammatory recovery process (Yung 2007, Mutsaers 2007).

PATHOPHYSIOLOGY OF EFFUSIONS

Normal body cavity fluid is a low protein blood ultrafiltrate derived from the arteriolar capillaries. Most of the fluid is resorbed into the venous capillaries while a smaller part is drained by the lymphatic system. The rate of fluid formation and reabsorption depends on Starling's forces, mesothelial and endothelial permeability, and the integrity of lymphatic drainage (Dempsey 2011).

Accumulation of fluid within a body cavity results from an impairment in the production and resorption systems. The fluid accumulates in case of increased capillary hydrostatic pressure, oncotic pressure gradient, endothelial permeability, interstitial hydrostatic pressure or with an ineffective lymphatic drainage.

Several disorders can produce this impairment, both acting locally (e.g., inflammatory or neoplastic process) or at distance (e.g., congestive heart failure). The presence of an excessive amount of fluid and the cytokine cascade induce a rapid activation of the local defence system comprising both immune and mesothelial cells. Additionally, in case of neoplastic diseases localizes to the serosal surface, neoplastic cells can exfoliate in the fluid. The number of shedding cells depends on the extension of the lesion and on their natural tendence to exfoliate, carcinomas, mesotheliomas, and round cell neoplasms exfoliate more readily than sarcomas (Dempsey 2011).

CLINICOPATHOLOGICAL CLASSIFICATION OF EFFUSIONS

Body cavity fluids are complex matrices with highly variable presentation in terms of aspect, chemical features, and number and type of cells. From a clinical point of view, they should be considered as a consequence of a pathological process rather than a primary disease. The analysis of the effusion allows the identification of the pathophysiological mechanism that produce the accumulation of the fluid itself. In some cases, it is also possible to determine the primary disease, or at least reduce the list of possible differential diagnoses. (Bohn, 2017; Cowell e Valenciano, 2014).

Traditionally effusions have been classified according to the underlying pathophysiologic mechanism in transudates, modified transudates, and exudates based on their cellularity and total protein concentration. A novel aetiological classification was described by O'Brien in 1988 and modified by

Stockham and Scott in 2008. This new scheme integrates the traditional numerical parameters with macroscopic and microscopic features creating a classification scheme more useful in clinical practice (Tab. 1-2).

Table 1. Cavitary effusions Pathologic processes, mechanisms, and conditions or disorders that produces effusions (Stokham and Scott 2008).

Pathologic process	**Pathologic mechanisms**	**Effusion**	**Conditions of disorders**
Transudation	Altered hydraulic and oncotic pressures	- Transudate, protein poor	- Cirrhosis, Protein-losing nephropathies and enteropathies, Lymphatic obstruction, Non-cirrhotic portal hypertension
Exudation	Increased vascular permeability to plasma proteins	- Transudate, protein rich	- Congestive heart failure, Portal hypertension (post sinusoidal)
		- Exudate, infections	- Bacteria, fungi, viruses, protozoa, and parasites
		- Exudate, non-infectious	- Neoplasia, foreign body, bile peritonitis, pancreatitis, steatitis, uroperitoneum, ischemic necrosis of spleen, lung, or other tissues due to torsion or vascular lesions
Haemorrhage	Leakage of blood from vessel	- Haemorrhagic effusion (acute)	- Trauma blood vessel, neoplasia, haemostasis defects
Lymphorrhage	Leakage of lymph from lymphatic vessel	- Haemorrhagic effusion (chronic)	- Neoplasia, haemostasis defect, trauma
		- Chylous effusion	- Cardiac disease, trauma, diaphragmatic lesions or hernia, neoplasms, and mediastinal lesions
		- Non-chylous lymphatic effusion	- Lymphatic obstruction
Rupture of hollow organ or tissue	Leakage of urine, bile, gastric or intestinal contents	- Secondary exudates infectious or non infectious	- Trauma, neoplasia, lithiasis, severe tissue lesion

Table 2. Common features of effusions (Stockham and Scott 2008). TP_{ref}, refractometric total proteins, TNNC, total nucleated cell count.

	Physical features	**TP_{ref} (g/dL)**	**TNCC (x 10^3/µL)**	**Predominant nucleated cells**	**Other findings**
Transudate, protein poor	Clear, colourless	<2.0	<1.5	Variable	Reactive mesothelial cells may be present
Transudate, protein rich	Clear to cloudy Yellow, orange, red	≥2.0	<5.0	Mostly neutrophils and macrophages	Reactive mesothelial cells are common
Exudate, bacterial or fungal	Hazy to cloudy Yellow, tan, cream, orange	≥2.0	>5.0	Neutrophils or neutrophils and macrophages	Bacterial may not be found via microscopy
Exudate, parasitic	Hazy to cloudy Yellow, tan, cream, orange	≥2.0	>5.0	Neutrophils or neutrophils and macrophages	Eosinophil percentages vary; parasite may not be found via microscopy
Exudate, non-infectious	Hazy to cloudy Yellow, tan, cream, orange, green	≥2.0	>5.0	Neutrophils or neutrophils and macrophages; Perhaps lymphocytes	
Haemorrhagic effusion, acute	Opaque Red	≥2.0	>2.0	Neutrophils and lymphocytes (most directly from blood)	Platelets is very recent haemorrhage
Haemorrhagic effusion, chronic	Hazy to opaque Red	≥2.0	>2.0	Neutrophils and macrophages	Erytrophages Siderophages
Chylous effusion	Hazy to white	≥2.0	<10.0	Small/Mixed leukocytes (long duration)	Sudanophilic droplets in fluid and macrophages
Lymphatic effusion	Hazy to cloudy Yellow to pink		<10.0	Small lymphocytes	
Uroperitoneum (initially)	Yellow	<2.0	<1.5	Variable	Urine crystals or sperm occasionally found
Uroperitoneum (persistent)	Variable	Variable	>1.5	Neutrophils and macrophages	Urine crystal occasionally found

STANDARD ANALISYS

As previously mentioned, standard effusion analysis includes a macroscopic examination of the fluid (colour and turbidity), the determination of certain biochemical features including the total protein concentration (TP) and other case-specific parameters (e.g., glucose, creatinine, bilirubin, triglycerides, cholesterol, lactate dehydrogenase). The corpuscular component of the fluid is quantitatively and qualitative assessed. Samples cellularity is estimated counting the total number of nucleated cells (TNCC) and red blood cell (RBCC). Traditionally cell counts were performed with manual counting chambers, but several studies demonstrated a good correlation between manual and automated counts performed with blood analysers (Gorman 2009, Pinto de Cunha 2009, Brudvig 2015).

The morphological evaluation of the cells plays a pivotal role in effusion analysis provides data regarding the underling pathological process, particularly when atypical cells are observed.

In addition, several ancillary test can be used to confirm, rule out, or refine the diagnosis based of the standard analysis. This is especially useful in terms of characterisation of the cells in fluid.

Automated Cell Count

Automation plays a pivotal role in high throughput diagnostic laboratories. Automated analysis has higher repeatability and reproducibility than manual systems, it is less operator dependent and allows fewer operators to manage higher numbers of samples at the same time.

A few studies have demonstrated that RBCC and TNCC can be reliably measured with two blood analysers (ADVIA 120, Siemens Healthcare; Sysmex it-2000iV, Sysmex Europe GmbH) in effusion fluid (Gorman 2009, Pinto de Cunha 2009, Brudvig 2015), also the effect of prolonged storage on these counts has been described (Maher 2010). Whereas, as reported in human medicine (Aules 2003), the accuracy of the differential counts of white blood cells was poor. This is likely due to the algorithms that these instruments use to identify the populations; they are designed to recognize standard populations in peripheral blood. Thus, if cells present slight morphological differences (e.g., activation, degeneration) or when other cell types are present (e.g., non-hematopoietic cells, NH) these algorithms fail to accurately recognize the populations. However, some cytogram patterns have been associated to the presence of specific cytologic findings, this may provide a tool to preliminary classify the effusions and identify atypical populations (Bauer 2005, Pinto de Cunha 2009). In particular, some cytogram patterns of ADVIA 120 suggesting the presence of specific cell types in the effusion have been proposed (Bauer 2005). These cytogram reading keys are summarized in table 8.

Cytology

Effusions cytology is considered one of the most challenging tasks for cytopathologist, especially in presence of atypical cells (Whitaker 2000, Davidson 2004, Politi 2005, Lin 2009, Shidham 2010).

Cytology has been demonstrated as a highly specific (99%) and poorly sensitive (64%) technique for canine neoplastic effusions (Hirschberger 1999). These performances are related to several factors. First, cells suspended in a fluid all have a round shape due to the surface tension. Thus, classification based on the shape of the cell is not possible in these samples. Although some cell types tend to exfoliate in aggregates, the cytologic architectural pattern poorly correlate with the tumour type (Bertazzolo 2012). Secondly, cell populations in effusions are a mix of inflammatory, reactive and neoplastic cells. The variable proportion of the different cell types may jeopardize the correct interpretation. Also, severe inflammation may affect the morphology of neoplastic cells making their identification harder (Mohanty 2003). Third, effusion fluid is an active environment, cells shed at different times and are therefore present at different activation and degeneration stages. Further, primary and several metastatic tumours may affect the body cavities, their high variability in terms of morphology further complicate the diagnosis (Davidson 2004, Politi 2005). Lastly, different cell types might present overlapping morphological features, this is particularly true for reactive mesothelial, epithelial and neoplastic mesothelial cells (Whitaker 2000, Baker 2000, Brisson 2006, Addis 2009, Ordonez 2006, Bertazzolo 2012).

Although these three populations represent the main diagnostic dilemma in effusion cytology, some cytologic features useful for diagnostics have been outlined. For instance, reactive mesothelial cells generally shed in low or moderate numbers, they tend to exfoliate individually or in small aggregates, the type and extent of the inflammatory component depend on the underlying mechanism of fluid accumulation. In case of persistent injury, mesothelial tissue become hyperplastic forming papillae supported by a collagen core. The apical portion of the papillae may detach, they can be seen in fluid cytology as round to papillary structures with a central bright pink core (stroma). Reactive mesothelial cells may present the brush border which appear in cytology as a pink cytoplasmic variably sized halo (Raskin 2015). Nuclei are round with stippled chromatin and often one or two prominent nucleoli. The cytoplasm moderate to abundant, often deeply basophilic, small round clear vacuoles may be seen (Geisinger 2004). Anisocytosis is mild to marked, anisokaryosis mostly mild to moderate. Mitotic figures, bi- and trinucleated cells are commonly found, and, in some cases, more atypical features such as multinucleation, karyomegaly, and anisonucleosis can also be present (Bolen 1986). Although reactive mesothelial cells may present severe malignancy criteria, only few of them are contemporary present and more frequently affect a small proportion of cells, if compared with their malignant counterpart.

Morphological features of neoplastic mesothelial cells are highly variable. Mesothelioma related effusions are often hypercellular, inflammation is generally mild, and the neoplastic cells predominate. Cells are highly pleomorphic, severe cellular, nuclear and nucleolar malignancy criteria are frequently observed. They affect the majority of the cells, and often, multiple criteria are seen in the same cell. On the contrary some cases show marked monomorphisms. Cells are medium to large, with high N:C

ratio, prominent nucleoli and hyperbasophilic vacuolated cytoplasm, and mild to moderate anisocytosis and anisokaryosis. Both predominantly single and cluster patters may be found (Raskin 2015). Additionally, several subtypes of mesothelioma have been recognized in human medicine, each with different morphological features, presentation, and behaviour (i.e., diffusion, shedding, localization) (Husain 2018).

Metastatic epithelial tumours are the most common non-haematopoietic tumours affecting body cavities (Raskin 2015). The morphology of metastatic epithelial cells is highly variable and depends on the degree of differentiation of the tumour and on the tissue of origin. Generally, they tend to exfoliate in large cohesive groups often with acinar and papillary architecture, however individualized cells are also present. These cells are mostly large in size, with variable N:C ratio, basophilic cytoplasm often with vacuolization which may be condensed in the perinuclear area. Secretory material can be seen within the cytoplasm in granules or condensed in large vacuoles. Nuclei are round, often paracentral to eccentric with stipple to coarse chromatin and multiple prominent nucleoli. Severe malignancy criteria are commonly found, atypical mitotic figures, marked anisocytosis and anisokaryosis, karyomegaly, and anisonucleosis are frequent, balloon and signet ring cells may be found (Raskin 2015, Cowell 2014).

Lastly, type three epithelial-to-mesenchymal transition (EMT) is further deemed responsible of morphologic changes that complicate the identification of cells in effusions. This theory has been suggested as a potential mechanism of carcinoma metastasis; cohesive neoplastic epithelial cell lose their polarization and stability and acquire migratory features typical of mesenchymal cells. From the diagnostic point of view, these changes, not only impact in cells morphology but also affect their immunoprofile. During EMT cells increase their expression of intermediate filaments typical of mesenchymal cells (i.e. vimentin) and underregulate the transcription of genes encoding for typical epithelial adhesion proteins (i.e. cadherins) (Dongre 2018).

Because of the high variability in the presentation and overlapping morphology of cells in effusions, a diagnostic approach known as "the third population" have been proposed (Shidham 2010). Assuming that inflammatory cells and reactive mesothelial cells are present in all effusion, this theory suggests to search for a "third population" of neoplastic cells. Even though both reactive mesothelial cells and neoplastic cells may display a wide spectrum of morphological features, there should be a subtle morphological continuum within the same cell type. This approach may help to differentiate neoplastic form non neoplastic cells, but do not allow the identification of the neoplastic cell type.

Cytological assessment is therefore mandatory for effusion classification, however, features inherent to the sample may limit the accuracy of the test, particularly in case of NH cells. To overcome these limitations, several ancillary tests have been developed to characterise cells in effusions.

ANCILLARY TESTS

Ancillary tests have been developed to improve the performances of cytology in effusion analysis and provide additional information to reduce the spectrum of possible differentials. These methods have been mainly focused on the identification of the cell types based on their immunophenotype.

Main limits of these techniques include the availability of antibodies specific for domestic species or that cross-react with them, the specificity of the antigen for a cell type, and the biological variability related to the activation status or neoplastic change of a cell. To overcome these limits, molecular techniques including genome sequencing are currently under study. However, an extensive application of these methods in the diagnostic setting is not yet feasible. Traditionally, immunocytochemistry on air-dried smears (ICC) was the most used ancillary technique. Recently, immunohistochemistry (IHC) on cell blocks have been and flow cytometry were introduced in the diagnostic routine also in veterinary medicine.

Immunocytochemistry and Immunohistochemistry

Immunocytochemistry consists in direct labelling on cytological preparation on air dried slides and it has been used for both diagnostic and research purposes in veterinary medicine (Ramos-Vara 2008). The main advantage is that allows the direct and contemporary visualization of cells morphology (with the details typical of cytology) and the immunolabelling, also it does not require expensive equipment (Raskin 2015). However, if compared with IHC on tissues, ICC show higher background and large clusters and thick smears cannot be assessed. Additionally, there are some technical disadvantages including the difficulty to obtain proper controls, to assess the slide quality before the staining, the high manual work required, and the lack of rapid standardizable protocols (Priest 2017). In the lasts years several studies tried to overcome some of these problems (Raskin 2019, Sawa 2017), however precise guidelines are still lacking particularly if compared with the decades-lasting experience of IHC on tissues.

IHC on tissues have a long history in both human and veterinary medicine, more antibodies are available, protocols are well known, and many laboratories are familiar with them. In the last years, the cell blocks, and old and forgotten technique, gained consideration also in veterinary medicine. This technique is an alternative cytological preparation that allows to apply immunohistochemical protocols and antibodies on cytological samples. Samples are prepared by condensing the cells in blocks which can be fixed, embedded, cut and stained as a tissue (Jain 2014). If compared with ICC, cell blocks allow to obtain several identical sections, to easily store the samples, and to study cells architectures. Hence, cell blocks make standard histological and immunohistochemical procedures accessible for cell suspensions with minimal need of protocols optimization (Saqui 2016). However, main disadvantages include the loss of typical cytological appearance, and the possible antigen loss due to fixation.

Additionally, IHC on cell blocks increases the turn-around time for each sample and requires laboratories equipped with tissue processing instruments.

Different methods and protocols have been investigated, some are based on direct fixation and centrifugation (Taylor 2013, Menezes 2016, Fernandes 2016), others use aggregation media such as agar (Zanoni 2012), gel foam (Wallace 2015) or specific polymers (Heinrich 2019). Among these methods the Agar-based Cell Block (ACB) seems adaptable to different samples and have a favourable cost/simplicity ratio. In human pathology, more than ten cell block methods are currently in use, being the ACB selected by 30% of the laboratories in the US (Crapanzano 2014).

Recently, a new medium-free technique known as Cell Tube Block (CTB) was described in veterinary medicine (Marcos 2017). This method requires only a small volume of fluid, and cells are concentrated and layered. This method stands out as a timesaving, easy to perform and cost-effective in particular for effusions samples (Marcos 2019)

Flow Cytometry

Flow cytometry is a method used to analyse cell suspensions. This method allows cell characterisation through their physical and fluorescence properties. In the flow cytometer, the cell suspension is channelled through a nozzle in a single-cell stream. Each cell passes a set of laser sources, while interrogated, the light scatter is measured by two optical detectors, one measure the light running along the path (forward scatter, FS) while the other measures the scatter at a ninety degree angle relative to the laser (side scatter, SS). These parameters reflect two morphological features of the cells: the size and the complexity. When measured in conjunction, these parameters allow, for some degree, to differentiate the cell types present in a heterogeneous population. Other lasers and detectors are used to detect fluorescent light (Shapiro 2003).

As in other immunobased ancillary techniques, antibodies are used in flow cytometry to detect antigens. Antibodies are directly or indirectly conjugated with florescent molecules, each detected at a different wavelength. Flow cytometric immunophenotyping is more frequently applied to detect surface protein, but cytoplasmic and nuclear antigens can also be identified. By direct measurement of the intensity of the signal the amount of antigen present in the cell can be estimated providing a quantitative objective measurement (in traditional techniques the amount of antigen is subjectively estimated semi-quantitatively). A major advantage of FC is the multicolour analysis. This allows to characterise several populations at the same time (Shapiro 2003, Ortolani 2019). The number of antibodies that can be contemporarily tested (up to 18) varies according to the types of lasers and detector that the flow cytometer is equipped with. From the technical point of view flow cytometry is rapid, less operator dependent, reproducible (the detection system is fully automated), and sensitive (thousands of cells

analysed). On the other side it requires fresh samples, and the costs of the instrument and specialized personnel are greater than of traditional methods.

In diagnostic clinical pathology, flow cytometry is widely recognized as a primary tool to refine the cytological diagnosis of lymphomas and leukaemias (Gelain 2008, Comazzi 2011, Rout 2017). It has been applied to several biological fluids (peripheral blood, bone marrow, cavitary effusions, cerebrospinal fluid) and tissue aspirates (lymph node, spleen, liver) (Duque 2002, Weiss 2002, Villiers 2006, Martini 2018). Although cells suspensions are samples perfectly suitable for flow cytometry, the role of this technique in effusion analysis and particularly for NH cells has not been fully investigated.

Recent studies, in human medicine, demonstrated that flow cytometry can contribute to refine the diagnosis of NH disorders in cavitary effusion. However, this is still a hot topic and no standard protocols have been defined (Davidson 2016, Pillai 2016).

NON-HEMATOPOIETIC CELLS IN EFFUSIONS

The presence of NH cells in cavitary effusions is due to exfoliation during benign (reactive mesothelial hyperplasia) or malignant (primary or metastatic tumours) processes. Exfoliation of reactive mesothelial cells non-specifically is secondary to any process that disrupt the normal body space homeostasis. On the other side, metastases of epithelial tumours are the most common cause of neoplastic exfoliation of NH cells in dogs. Whereas mesotheliomas and sarcomas and are less frequent (Raskin 2015). As described above, the morphologic differentiation of these cell types is challenging and immunophenotyping is often needed when suspicious NH cells are observed in cytology.

As suggested by Dabbs in 2006, the first step for immunochemical characterisation of cells should include markers able to distinguish the major cell lineages. This would include CD45 (leukocytes), pancytokeratin (epithelial and mesothelial cells), and vimentin (mesenchymal and mesothelial). Major markers can identify the lineage in the majority of the cases, however there are well known exceptions such as the lack of CD45 expression in T-Zone lymphomas. Further, due to the inherent nature of neoplastic diseases phenotypic aberrancies can mislead immunoprofiles interpretation. Therefore, the choice of the antibodies and their interpretation should always rely on the morphology of the cells. Once the major lineage is established, specific antibodies may used to identify specific subgroups. For example, CD79 and CD3 to determine the B or T lineage of lymphoid cells and, among T-cells, CD4 and CD8 subsets. This algorithm is well established for hematopoietic cells, while it is less known for NH cells in effusions. In these cases, broader panels are used in humane medicine often including expected positive and negative markers (Husain 2018). However, in veterinary medicine the availability of board panels of antibodies for specific NH subset is limited.

Non-Hematopoietic cells characterisation

Intermediate filaments are the best candidates for major lineage characterisation. They are the essential component of the cytoskeleton and provide plasticity, stability, and anchor cytoplasmic organelles. Being structural component of the cells, they are generally conserved also after neoplastic change, thus, are reliable marker to determine the origin of cancer cells. They are expected to be highly expressed providing a diffuse and strong immunohistochemical staining pattern in most of the cells.

Cytokeratins are a broad family of intermediate filaments expressed in most normal and neoplastic epithelial and mesothelial cells. They are connected with desmosomes, and actively participate to maintain the integrity of the tissue. Cytokeratins include more than twenty molecules divided in low and high molecular weight, different profiles are expressed in epithelial cells according to their organ of origin. To ensure a broad detection of cytokeratins a cocktail of two antibodies is used in diagnostic pathology, this is able to identify both low (CK AE1) and high (CK AE3) molecular weigh proteins.

On the other side vimentin is an intermediate filament that primary identify cells of mesodermal origin. It has been related to the maintenance of the cell shape, and it is expressed in both benign and malignant mesenchymal tissues and in mesothelial cells (Afify 2002, Reggeti 2005). It is also present in neutrophils, macrophages (Mor-Vaknin 2003) and lymphocytes (Bilalic 2012).

Although, in general, cytokeratin identifies epithelial cells while vimentin expression supports a mesenchymal origin, in diagnostic pathology their coordinate expression occupies a more relevant role. Cytokeratin and vimentin are coexpressed in both benign and malignant mesothelial cells (Ferrandez-Izquierdo 1994, Afify 2002.) and they have been largely used for diagnostic purposes on effusion samples in both dogs and cats (Geninet 2003, Reggeti 2005, Sato 2005, Morini 2006, Vascellari 2011, Przezdzieki 2014, D'angelo 2014, Wallace 2015, Milne 2017, Sawa 2018, Marcos 2019). However, recent studies have demonstrated that human mesothelial cells are capable of deep morphological and phenotypical changes (Mutsaers 2004, Yung 2009) and that they can undergo to epithelial-to-mesenchymal transition when activated or when adapting to new conditions (Yenez-Mo 2003). Further, vimentin has been reported as inconsistent in staining canine mesothelial cells (Marcos 2019). Additionally, several other neoplastic and non-neoplastic tissues have been demonstrated coexpressing those two markers including anaplastic carcinomas, amelanotic melanomas, renal carcinomas, Sertoli cell tumours, thyroid carcinomas, prostatic carcinomas, endometrial adenocarcinoma, ovarian epithelial tumours, mammary gland carcinomas (Grieco 2003, Reggeti 2005, Riccardi 2007, Pires 2010) and in nearly 40% of canine primary lung tumour (Burgess 2009). For all these reasons additional markers for mesothelial cells identification have been proposed in human medicine. Guidelines suggest the use of a minimum of eight antibodies (four expected positive and four expected negative) in the panel to confirm the histological suspect of mesothelioma (Husain 2018). Few markers have been tested in IHC in dogs for the same purpose, these include EMA (Sato 2005), Calretinin (Geninet 2003, Sato 2005,

Morini 2006, D'angelo 2014), HBME-1 (Machida 2004), WT1 (Sato 2005, Vascellari 2011, D'angelo 2014, Marcos 2019), GLUT1, IMP3 (Milne 2017) and Desmin (Morini 2006, Milne 2017).

Desmin is an intermediate filament express by normal smooth and skeletal tissues and their neoplastic counterparts. The specific function is still unknown, but it is variably expressed in the different cell types during their differentiation. Desmin expression has also been demonstrated in non-myogenous tumours such as neuro-ectodermal tumours and, rarely, in some carcinomatous effusions in humans with a faint staining in a low proportion of cells. (Gill 2000, Davidson 2001). Several studies reported a positive reaction in benign mesothelial cells in human serous fluid and tissue sections (Gill 2000, Davidson 2001, Su 2010, Hasteh 2010, Dabbs 2006). Further, desmin has been found a useful marker (84% Se, 94% Sp) to identify reactive mesothelial cells in cytologic effusion specimens (Hasteh 2010). Still, the reason of desmin expression in reactive mesothelial cells is unknown, some studied proposed the multipotential role with possible muscle differentiation (Bolen 1986, Afify 2002).

In veterinary medicine results are less consistent, although negative in two reported malignant mesotheliomas (Morini 2006, Sato 2005), it seems specific for mesothelial origin but not able to distinguish between reactive and neoplastic mesothelial cells in effusions (Hoingaus 2008, Przezdziecki 2014), while it inconsistently stained mesothelial cells in pericardial tissue (Milne 2017).

AIM

The aim of this PhD project was to investigate the application of diagnostic ancillary techniques in canine cavitary effusions analysis with particular interest in non-hematopoietic cells.

The project has been developed in three sections, each with specific goals:

1. Identify the best cell block method in terms of morphology and immunohistochemical staining, considering also technical and practical aspects of a diagnostic laboratory.
2. Assess the diagnostic performances of the interpretation of the cytogram patterns of an automated analyser (ADVIA 120) in the diagnosis of canine pleural, peritoneal, and pericardial effusions.
3. Develop a flow cytometric strategy able to identify non-hematopoietic cells in canine effusions and characterise them with major lineage markers.

1. CELL BLOCKS

1.1 INTRODUCTION

Cell blocks are an alternative cytological preparation were cells are concentrated in a block that can be processed as tissue. Fluid-to-solid conversion techniques have been increasingly reported in veterinary literature; however, protocols are often retrieved from human studies. Therefore, methods optimization on veterinary samples is warranted and would contribute to include these specimens in the diagnostic routine workout. According to the literature, two methods seems to comply with the technical need of diagnostic laboratories and at the same time seems able to provide reliable results.

In this part of the study, agar-based cell blocks (ACB) and cell tube blocks (CTB) were prospectively compared in terms of morphological and immunohistochemical features. Further, practical aspects useful for its introduction in diagnostic setting were considered.

1.2 MATERIALS AND METHODS

Canine and feline pleural, pericardial and peritoneal effusion fluids were collected at the Clinical Pathology Laboratory of the University of Turin (IT) and at the Cytological Diagnostic Services of the Institute of Biomedical Sciences Abel Salazar (ICBAS-UP), University of Porto (PT) in two consecutive periods. All patients were privately owned and sampled for diagnostic purposes.

Only samples with at least 2 ml of fluid in EDTA left after routine processing where included. Inclusion criteria were: (1) presence of neoplastic/atypical cells in cytology and/or (2) packed cell volume ≥3%. The available volume of fluid was split in two equal parts and processed by the same operator within 24 hours from collection with the ACB and CTB methods.

Cell block preparation, processing, and evaluation

Agar based cell blocks were prepared with two different aggregation media following the standard operating procedures of the two centres. In the laboratory of Turin, Bio-Agar™ (Bio-Optica, Milano, IT) was used, while HistoGel™ (Thermo Fisher Scientific, Waltham, MA) was used in Porto. After spinning samples at 1200 rpm for 5 minutes the cell pellets were fixed in formalin for 24 hours. Afterwards, the pellets were gently stirred with an equal volume of melted aggregation medium, after cooling, it was removed from the tube, placed in cassettes, and processed for routine histology.

CTB were prepared following the technique described by Marcos in 2017. The sample was introduced in plain capillary tubes, sealed with clay, and centrifuged in a microhematocrit centrifuge at 12700g for 5 minutes. To ensure a final length of the pellet between two and five millimetres, poorly cellular samples were previously concentrated by centrifugation. In cases where red blood cells (RBC) where not visible, a high-density solution (Percoll™, Sigma-Aldrich, St Louis, USA) was added, as described in

the original technique, to ensure few millimetres of separation between the pellet and the clay. Once centrifuged, capillary tubes were cut at the liquid-solid interface, fixed in formalin for 24 hours, placed in a cassette and routinely processed as histological samples. After processing, the material was removed from the tube and embedded. Three micrometre sections were placed on precoated slides and stained with H&E for morphological evaluation.

The presence of residual materials in the background was evaluated by two observers in a multi-headed microscope. Residual materials included materials derived form the technique such the aggregation media and the clay or inherent to the sample as fibrin strands, basophilic granular-fibrillar material, granular proteinaceous material, deeply basophilic strands of nuclear material, and formalin pigment.

Virtual Slide Microscope VS110 (Olympus, Tokyo, Japan) was used for slides digitalization. Two rectangular areas of similar size of each slide were depicted concealing the shape and digitalized. Scanning was performed with Multi Z-layer focus mode with a 20x objective, which ensures a view up to 60x magnification with digital zoom. Images were evaluated by an experienced cytopathologist with OlyVIA 2.4 (Olympus Life Science, Tokyo, Japan), a software optimized for digital pathology. The observer was blind to technique used and assessed general appearance features (cellularity and RBC separation) (Tab.3) and the presence of the following cellular features were assessed: cellular arrangements (single cell, groups without a defined architecture, groups with a defined architecture), cell types and prevalent cell population (polymorphonuclear cells, macrophages, lymphoid cells, mesothelial cells, suspicious neoplastic non-lymphoid cells) and cellular artifacts (shrinkage, ground glass appearance, nuclear meltdown, frayed cytoplasmic borders).

Table 3. Score-system for evaluation of general appearance and immunohistochemical features of cell blocks from canine and feline cavitary effusions.

	Score		Description
General appearance			
Cellularity	0	Acellular	Absence of nucleated cells
	1	Low	Rare and scattered nucleated cells
	2	Medium	Moderate amount of nucleated cells, fields with empty areas
	3	High	Abundant nucleated cells, all fields filled with nucleated cells
RBC separation	1	No separation	RBC and nucleated cells are completely mixed
	2	Partial	Most RBC are separated, several RBC are present among nucleated cells
	3	Complete	Most RBC separated, rare or no RBC are present among nucleated cells
Immunohistochemistry			
Staining intensity	1	Weak	Referred to controls
	2	Moderate	Referred to controls
	3	Strong	Referred to controls
Background	0	Absent	No background staining, clear spaces between cells
	1	Low	Slight background, easy interpretation
	2	Moderate	Evident presence of background, evaluation possible but could interfere with weak specific signals
	3	High	Positive cells and background have similar intensity, difficult evaluation

Immunohistochemistry

Routine protocols for formalin-fixed paraffin embedded tissues were used for immunohistochemical staining. To ensure similar staining conditions, paired ACB and CTB sections were stained in the same run. Previously titrated monoclonal antibodies against pan-cytokeratin (CK, clone CK AE1/AE3, dilution 1:1000; Cell-Marque, Sigma-Aldrich, Rocklin, CA) and vimentin (VIM, clone V9, dilution 1:1600, Novocastra, Leica Biosystems Newcastle, UK) were used. Heat induced antigen retrieval was used in a slightly acid solution (water bath in citrate solution, pH 6.5, 100°C) and Novolink Polymer Detection System (Leica Biosystems Newcastle, UK) was used. The used chromogen was Diaminobenzidine and Harris haematoxylin was used to counterstain. In each run, canine intestine sections and omission of primary antibody were used as positive and negative controls. Two observes evaluated the slides in a multiheaded microscope, the immunohistochemical scoring was the result of a consensus between the two. Evaluated parameters are summarize in table 3, further the presence of nonspecific staining of residual background materials was recorded.

Data Analysis

Statistical analyses were performed using IBM SPSS Version 23.0 (IBM Corp. Armonk, NY, USA). Within each method, scores of specimens collected in the two centres were homogeneous and cases were grouped together for the rest of the analysis. Overall yield was calculated as proportion of cases providing evaluable sections. Features of residual background materials in H&E and IHC stained slides were descriptively analysed. ACB and CTB scores for cellularity, RBC separation and IHC staining intensity were compared with Wilcoxon test. Concordance of the two methods in identifying the same architectural patterns, cell types and the prevalent cell population was expressed as percent agreement. Statistical comparisons between methods or within methods between haemorrhagic and non-haemorrhagic cases were performed for nominal data using Fisher`s exact test and for ordinal data using the Mann-Whitney U test. A 5% level was considered to define statistical significance for all tests.

1.3 RESULTS

Fifty-two spontaneous cavitary effusions from 39 dogs and 13 cats were included. Effusions were from pleural (n=17 and n=8, in dogs and cats respectively), peritoneal (n=8 and n=3), and pericardial (n=14 and n=2) cavities. Twenty-three samples were collected in the Turin and 29 in Porto B. Twenty-five samples were classified as haemorrhagic. Median total nucleated cell count was 9.4 (1.5 - 48.7, interquartile range 22.6) $x10^3$ cell/uL.

Overall yield

The overall yield was 100% (52/52) for ACB and 98% (51/52) for CTB. The unsuccessful CTB was a haemorrhagic sample (packed cell volume=13%) without neoplastic/atypical cells, in which the cell pellet (2 mm long) was lost during the embedding.

Residual background materials

Residual background materials were observed in both ACB and CTB; details on frequency and distribution are shown in Tab.4, and Fig.1. In ACB, Bio-Agar™ and HistoGel™ surrounded the cell pellet and formed lakes among the cells. Basophilic granular-fibrillar material and granular proteinaceous material were diluted, scattered, and mixed with cells. Areas without or at least with minimal amount of those materials were often present. Fibrin strands occasionally entrapped few nucleated cells. In CTB, residual clay was observed in few cases. Granular proteinaceous material and basophilic granular-fibrillar material were layered at the top of the CTB, completely or partially separated from the cells, while fibrin strands did not layer in any specific position but were gathered together. Other background materials were infrequently observed. Overall background materials did not affect the morphology of the cells, but lengthen the time needed for slide evaluation.

Table 4. Frequencies and distribution of residual background materials in cell blocks prepared from canine and feline cavitary effusions.

	Agar Cell Blocks (n=51)		**Cell Tube Blocks (n=51)**	
	n (%)[a]	**Distribution, n (%)[b]**	**n (%)[a]**	**Distribution, n (%)[b]**
Bio-Agar™/ HistoGel™	37 (72.5)	Mixed, 37 (100)	na	na
Clay	na	na	4 (7.8)	Bottom layer, 3 (75) Partially mixed, 1 (25)
Granular proteinaceous	8 (15.6)	Mixed, 8 (100)	26 (50.9)	Top layer, 22 (84.6) Partially mixed, 4 (15.3)
Basophilic granular-fibrillar	19 (37.2)	Mixed, 19 (100)	5 (9.8)	Top layer, 3 (60) Partially mixed, 2 (40)
Fibrin strands	11 (21.5)	Scattered, 11 (100)	7 (13.7)	Scattered, 7 (100)
Deeply basophilic nuclear	3 (5.8)	Scattered, 3 (100)	1 (1.9)	Top layer, 1 (100)
Formalin pigment	1 (1.9)	Localized, 1 (100)	4 (7.8)	Bottom layer 4 (100)

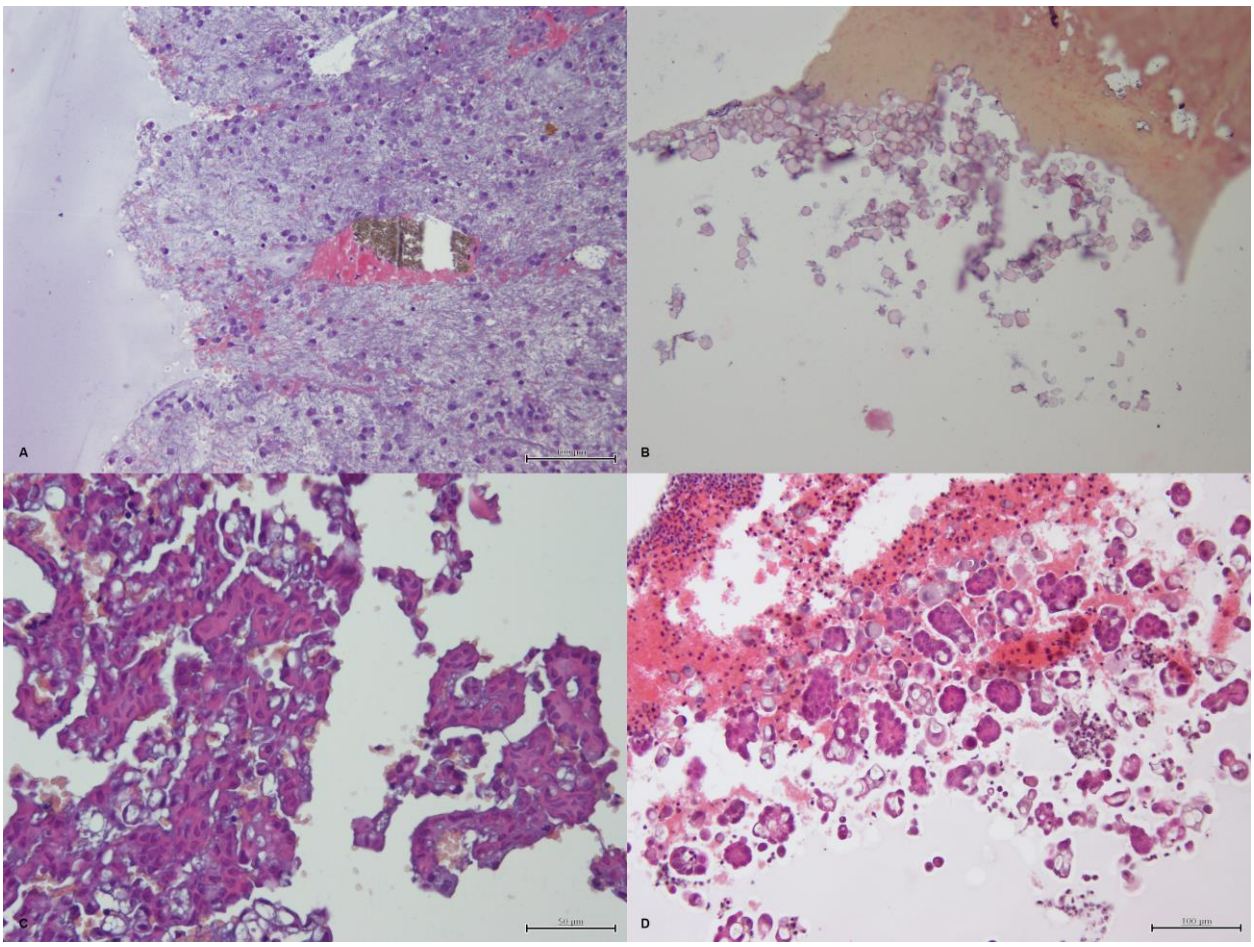

Figure 1. Residual materials and cellular artifacts observed in agar cell blocks and cell tube block obtained from canine and feline cavitary effusions. **A**, Dog, abdominal effusion, agar cell block. On the left, light blue to greyish homogeneous material (HistoGel™). On the right, basophilic granular-fibrillar material mixed with cells and formalin pigment (black fine pigment with goldish reflects is localized in a lacuna of RBC), H&E, x20 objective. **B**, Dog, pleural effusion, cell tube block. Clay, round to polygonal refringent unstained crystal-like material with a darker inflection in the centre localize at the bottom layer, H&E, x20 objective. **C**, Cat, pericardial effusion, cell tube block. Ground glass appearance and nuclear meltdown, H&E, x40 objective. **D**, Cat, pleural effusion, agar cell block, shrinkage, H&E, 40x objective.

General appearance and cellular features

Overall, CTB had scores of cellularity and RBC separation significantly higher than ACB ($p<0.001$). In particular, half of the ACB displayed low cellularity (score 1), while the majority of CTB had high cellularity (score 3) (Tab.5). Similarly, RBC were mixed (score 1) with the cells in the majority of ACB, while they were mainly, completely (score 3) or partially (score 2), separated from nucleated cells in CTB (Tab.5). Within each technique, no significant differences were detected for cellularity and RBC separation scores when comparing haemorrhagic and non-haemorrhagic samples (Tab.6).

ACB and CTB had a high overall concordance (>93.8%) in identifying cellular arrangements, cell types and prevalent population. Cellular artifacts were observed in 22/51 (43.1%) CTB and in 18/51 (35.3%) ACB. In CTB, cells presented flat, hazy and with uniform cytoplasm (ground glass appearance) in 15/51 (29.4%) cases and poorly defined chromatin and a blue haze effect (nuclear meltdown) in 10/51 (19.6%) cases. In 9 of those, the two alterations coexisted, and, in all cases, they had a patchy distribution within the section. In ACB, ground glass appearance (4/51, 7.8%) and nuclear meltdown (1/51, 2%) were present, but in a significantly lower proportion of cases ($p=0.009$ and $p=0.008$ respectively). Shrinkage frequently affected single and isolated cells and was observed in 9/51 (17.6%) CTB and in 15/51 (29.4%) ACB. Frayed cytoplasmic borders were rare in both CTB (1/51, 2%) and ACB (2/51, 3.9%). Ground glass appearance and shrinkage were observed in matched CTB and ACB in a single case. ACB were mainly affected by one (15/18, 83.3%) defect at a time, while in half of the CTB cases (12/22, 54.5%) multiple defects were contemporarily present ($p=0.021$). (Fig.1)

Table 5. Frequencies[a] of scores of general appearance and immunohistochemical features of cell blocks from canine and feline cavitary effusions.

General appearance					
Score	**0**	**1**	**2**	**3**	
Cellularity[b]	**Acellular**	**Low**	**Medium**	**High**	**Total**
ACB	0 (0)	25 (49)	16 (31.3)	10 (19.6)	51 (100)
CTB	0 (0)	2 (3.9)	13 (25.5)	36 (70.6)	51 (100)
RBC separation[b]		**No separation**	**Partial**	**Complete**	**Total**
ACB		40 (78.4)	9 (17.7)	2 (3.9)	51 (100)
CTB		1 (2)	26 (51)	24 (47)	51 (100)

Immunohistochemistry					
Score	**0**	**1**	**2**	**3**	
Intensity CK		**Weak**	**Moderate**	**Strong**	**Total**
ACB		0 (0)	2 (4.1)	47 (95.9)	49 (100)
CTB		0 (0)	2 (4.1)	47 (95.9)	49 (100)
Intensity VIM		**Weak**	**Moderate**	**Strong**	**Total**
ACB		0 (0)	7 (14.3)	42 (85.7)	49 (100)
CTB		0 (0)	4 (8.2)	45 (91.8)	49 (100)
Background CK[c]	**Absent**	**Low**	**Moderate**	**High**	**Total**
ACB	28 (57.1)	15 (30.6)	6 (12.3)	0 (0)	49 (100)
CTB	42 (85.7)	5 (10.2)	2 (4.1)	0 (0)	49 (100)
Background VIM	**Absent**	**Low**	**Moderate**	**High**	**Total**
ACB	39 (79.6)	8 (16.3)	2 (4.1)	0 (0)	49 (100)
CTB	38 (77.6)	10 (20.4)	1 (2)	0 (0)	49 (100)

[a] values expressed as absolute numbers, proportions over total in parenthesis; [b] significantly higher scores in CTB than ACB ($p<0.001$, Wilcoxon signed-rank test); [c] significant association between

Table 6. Cellularity and RBC separation scores of cell blocks from haemorrhagic (n=24) and non-haemorrhagic (n=27) canine and feline cavitary effusions.[a]

	Agar Cell Blocks			**Cell Tube Blocks**		
CELLULARITY	**Low**	**Medium**	**High**	**Low**	**Medium**	**High**
Score	**1**	**3**	**3**	**1**	**2**	**3**
Haemorrhagic	12 (50)	8 (33.4)	4 (16.6)	2 (8.4)	5 (20.8)	17 (70.8)
Non-haemorrhagic	13 (48.2)	8 (29.6)	6 (22.2)	0 (0)	8 (29.6)	19 (70.4)
RBC SEPARATION	**No separation**	**Partial**	**Complete**	**No separation**	**Partial**	**Complete**
Score	**1**	**3**	**3**	**1**	**2**	**3**
Haemorrhagic	19 (79.2)	5 (20.8)	0 (0)	1 (4.2)	12 (50)	11 (45.8)
Non-haemorrhagic	21 (77.8)	4 (14.8)	2 (7.4)	0 (0)	14 (51.9)	13 (48.1)

[a] values expressed in absolute numbers, proportions over total in parenthesis

Immunohistochemistry

One non-haemorrhagic sample with neoplastic/atypical cells was excluded due to CTB over-sectioning when preparing slides for IHC. Thus, IHC was performed in 50/51 CTB cases. Forty-nine out of 50 cases yielded evaluable IHC stained sections. One CTB section did not resist to the immunostaining protocol. In the background, granular material and basophilic granular-fibrillar material showed variable nonspecific staining of weak intensity. Nevertheless, the interference with the evaluation was minimal because of their localization and distribution within the section (as detailed above).

IHC for CK and VIM showed similar staining intensity in paired ACB and CTB. CK and VIM staining intensity was always cytoplasmic and strong (score 3) in almost all the cases in both ACB and CTB, and no weak staining intensity (score 1) was observed (Tab.3). Nonspecific background was present in a significantly higher proportion of cases in ACB (20/49, 40.8%) than CTB (7/49, 14.3%) when stained with CK ($p=0.006$), while it was similar in VIM stained sections (10/49, 20.4% and 11/49, 22.4% respectively). When present, the nonspecific background had low intensity (score 1) in both CK and in VIM stained ACB (15/20, 75% and 8/10, 80%) and CTB (5/7, 71.4% and 10/11, 90.9%) (Tab.5). In the remaining cases nonspecific background had moderate intensity (score 2), but no strong intensity (score 3) was observed. Haemorrhagic and non-haemorrhagic samples did not show significant differences for IHC staining intensity and background scores (Fig.2 and Tab.7). Likewise, no differences were noted in material collected in the two centres.

Technical aspects

CTB and ACB were produced with basic equipment available in a pathology laboratory using both consumable and specific materials (HistoGel™ and Bio-Agar™) with negligible and low costs (≈1€ and ≈3€ per sample for CTB and ACB, respectively).

Training of unskilled personnel for ACB and CTB preparation included less than 1 hour of training with a brief practical demonstration. Correctly prepared CTB were immediately obtained, while melting and mixing the aggregation media were the main difficulties encountered in ACB preparation. Regarding processing phase, ACB did not required any specific training, while for CTB a 2 hours training followed by few days of practice was needed to obtain optimal results.

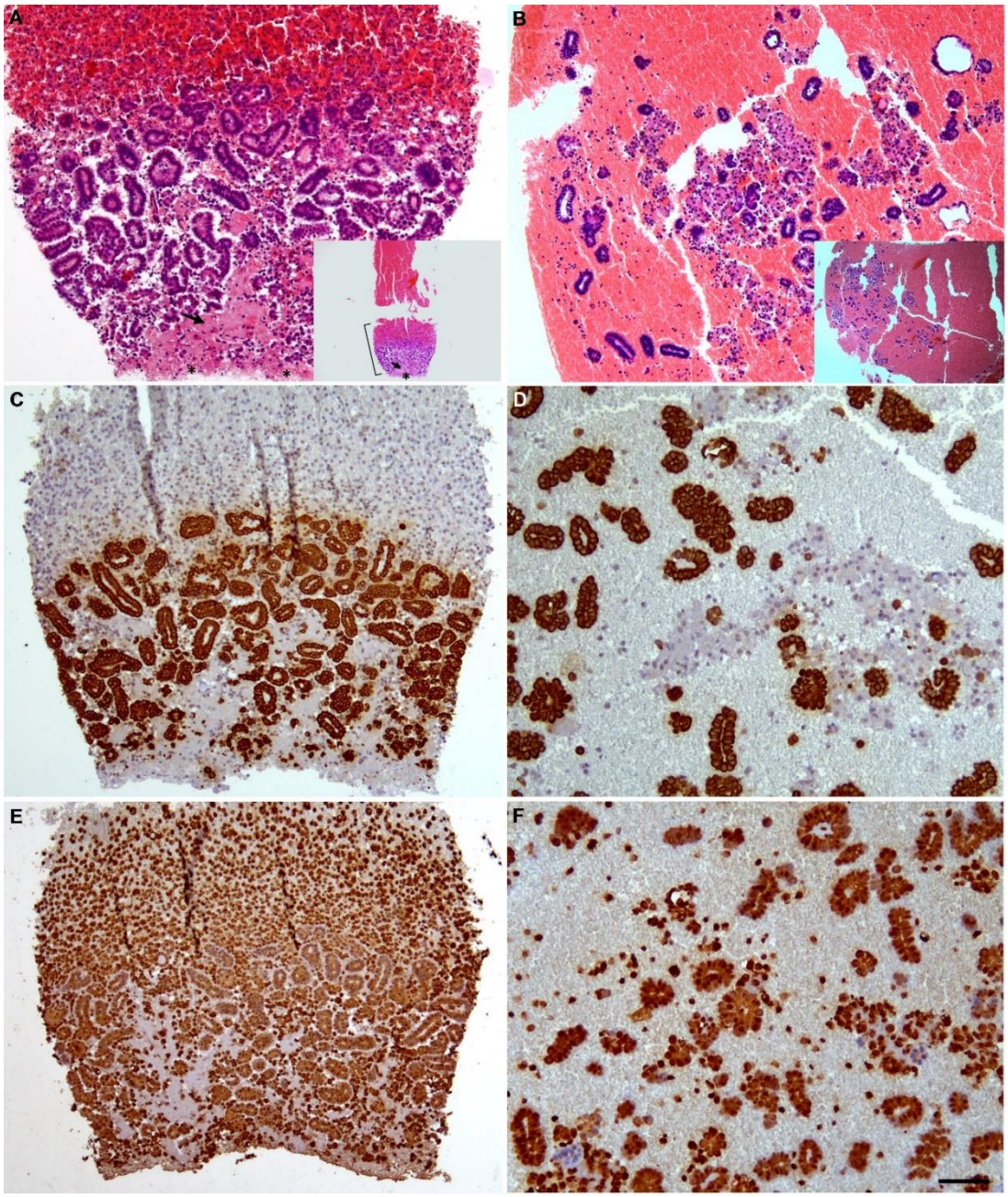

Figure 2. Dog, pericardial effusion with mesothelial hyperplasia. Cell tube block (A, C, E) and agar cell block (B, D, F). A, RBC are mostly separated from nucleated cells which are condensed in a small area (bracket), groups of mesothelial cells, fibrin strands (arrows) and granular proteinaceous material (*) are localized at the top of the pellet, H&E, bar = 140 µm (inset 1000 µm). B, mixture of RBC, inflammatory and mesothelial cells (single or in groups); fibrin strands appeared mixed with these elements (not highlighted in this picture), H&E, bar = 140 µm (inset 1000 µm). C, D, mesothelial cells with papillary architecture and few scattered large mesothelial cells have strong immunoreaction for pan-cytokeratin, without background non-specific staining. Diaminobenzidine chromogen, Hematoxylin counterstained (bar = 140 µm). E, F, inflammatory cells have strong immunoreaction for vimentin, whilst mesothelial cells with papillary architecture and few scattered mesothelial cells are also positive, without non-specific background staining. Note that inflammatory cells negative to pan-cytokeratin and positive to vimentin appear clearly layered in the cell tube block (upper half of C and E). Diaminobenzidine chromogen, Hematoxylin counterstained, (bar = 140 µm).

Table 7. Immunohistochemical staining intensity and background scores of cell blocks from haemorrhagic (n=24) and non-haemorrhagic (n=25) canine and feline cavitary effusion. [a] values expressed in absolute numbers, proportions over total in parenthesis

PAN-CYTOKERATIN

	Agar Cell Block				**Cell Tube Block**			
Intensity		**Weak**	**Moderate**	**Strong**		**Weak**	**Moderate**	**Strong**
Score		**1**	**2**	**3**		**1**	**2**	**3**
Haemorrhagic		0 (0)	0 (0)	24 (100)		0 (0)	2 (8.3)	22 (91.7)
Non-haemorrhagic		0 (0)	2 (8)	23 (92)		0 (0)	0 (0)	25 (100)
Background	**Absent**	**Low**	**Medium**	**High**	**Absent**	**Low**	**Medium**	**High**
Score	**0**	**1**	**2**	**3**		**1**	**2**	**3**
Haemorrhagic	13 (54.2)	6 (25)	5 (20.8)	0 (0)	19 (79.1)	3 (12.5)	2 (8.3)	0 (0)
Non-haemorrhagic	16 (64)	8 (32)	1 (4)	0 (0)	23 (92)	2 (8)	0 (0)	0 (0)

VIMENTIN

	Agar Cell Block				**Cell Tube Block**			
Intensity		**Weak**	**Moderate**	**Strong**		**Weak**	**Moderate**	**Strong**
Score		**1**	**2**	**3**		**1**	**2**	**3**
Haemorrhagic		0 (0)	3 (12.5)	21 (87.5)		0 (0)	0 (0)	24 (100)
Non-haemorrhagic		0 (0)	4 (16)	21 (84)		0 (0)	4 (16)	21 (84)
Background	**Absent**	**Low**	**Medium**	**High**	**Absent**	**Low**	**Medium**	**High**
Score	**0**	**1**	**2**	**3**		**1**	**2**	**3**
Haemorrhagic	18 (75)	4 (16.7)	2 (8.3)	0 (0)	16 (66.7)	7 (29.2)	1 (4.1)	0 (0)
Non-haemorrhagic	21 (84)	4 (16)	0 (0)	0 (0)	22 (88)	3 (12)	0 (0)	0 (0)

1.4 DISCUSSION AND CONCLUSION

Recently cell blocks have gain interest in veterinary cytology, especially for immunohistochemical studies on different matrices (Zanoni 2012, Taylor 2013, Wallace 2015, Menezes 2016, Fernandes 2016, Marcos 2017, Marcos 2019, Heinrich 2019). Their increasing use is likely related to an increasing interest in immunobased ancillary techniques in diagnostic clinical pathology and the fact that they are not expensive and have minimal impact on laboratory workflow. In this vein, two cell block methods were selected for their simplicity, limited cost, and speediness, to explore technical issues and compare their morphological and immunohistochemical features.

Both investigated methods displayed a high yield and were able to provide good quality sections for IHC in almost all cases. Results were excellent especially if compared with the moderate success and satisfaction rates reported in human medicine for agar-based methods (Crapanzano 2014, Jain 2014). Immunohistochemistry results were straightforward, with a strong positive reaction for all samples independently from the centre where they have been collected and the method used. CK stained ACB showed a higher nonspecific background than CTB, however, when present its intensity was generally of low and did not affect the final interpretation. Probably this higher occurrence is related to the presence of residual background materials (granular and basophilic granular-fibrillar). Despite their presence, those materials were often diluted and fields free of this material could be easily encountered. Conversely in CTB, those materials did not contribute to the background because they were layered and separated from nucleated cells. These results confirm that cell blocks are reliable for IHC studies on effusion samples (Fetsch 2002, Wallace 2015, Marcos 2017, Marcos 2019) and suggest that routine IHC procedures used for tissue biopsies can be directly transferred to CB.

Although both methods provided excellent results, observed differences can be beneficial depending on the specific need. For example, nucleated cells in CTB are densely packed in a small area and well separated from RBC. Those features would be most useful in haemorrhagic samples, where cells of interest are highly diluted, ensuring a faster and straightforward evaluation of nucleated cells. An additional advantage of CTB is that they allow to contain the staining area reducing the waste of reagents. Further, the majority of RBC are removed before embedding, making the paraffin block easier to section compared to RBC-rich ACB. Despite ACB protocol also includes a centrifugation step, cells are less condensed, heterogeneously distributed, and variably mixed with RBC. Indeed, the effects on cellularity and RBC separation in ACB are highly operator-dependent, and thus difficult to standardize.

Samples with variable cellularity were included in the study. The sample with the lowest cellularity had $1.5x10^3$ cells/uL and the available volume of fluid was 1 mL for each technique. Thus, as a general indication, 1 ml of fluid with at least $1.5x10^3$ nucleated cells/uL is likely to results in a good cell block with both methods.

Similar cellular artifacts were observed in both methods. Although the actual origin of nuclear meltdown is unclear (Rolls 2010) a slower penetration of processing solutions in the capillary tube can justify their higher prevalence in CTB. Other suggested tissue-related causes are unlikely in these cases; indeed, those artifacts were absent in the majority of matched ACB. ON the other side, cells in ACB were more frequently shrink than in CTB, the origin of this phenomenon has hypothesized as the result of a heat damage induced by melted aggregation media (Jain 2014). Even though other causes of shrinkage cannot be ruled out, the effect of normal paraffin shrinkage might be enhanced in cell block material comparing with tissues. Indeed, isolated small cells seem more affected while the higher cohesiveness of CTB appears to reduce its occurrence. Even though cellular artifacts have occurred, their patchy distribution and mild severity did not jeopardize the overall morphological interpretation. Immunohistochemical features were not affected by these artifacts, however, when not well-established markers are being used for the first time in cell blocks, results should be interpreted cautiously in presence of these artifacts.

ACB and CTB are highly concordant in the identification of cellular architecture and cell types in paired samples, however, CTB cell layering facilitate the identification of different populations providing additional value to the technique when rare cell populations are present (Marcos 2017). The identification of the sell type of each cell can be difficult, this is probably an effect of fixation, embedding and sectioning. This further confirms that cell blocks should never be used as an exclusive method for morphological evaluation and diagnosis, but as complementary preparation to be assessed alongside with conventional cytology (Jain 2014, Marcos 2017).

Additionally, technical issues should be considered when introducing a new method in routine practice. ACB and CTB can be prepared with basic equipment and consumables, overall costs are negligible or very low (in ACB they are mainly due to the cost of the aggregation media).

In terms of preparation, ACB are more time-consuming and needs more care in melting the medium at the right temperature. Moreover, samples are not prepared in batches but only occasionally, meaning that a higher volume of agar medium would be wasted, thus increasing the cost per-sample. On the other side, CTB protocol is simpler and minimal manual skills and expertise are needed. Additionally, in-clinic CTB preparation have been successfully demonstrated in previous studies (Marcos 2017). Although in this study all procedures were performed in the laboratory, it is likely that clinicians could be able to produce CTB directly in clinic and ship them to the laboratory while fixing. Reducing collection-processing interval would limit specimen degradation and speed up the following processing procedures.

In the second phase of their production, cell blocks are included in the routine histology workflow of the laboratory without additional dedicated time. In this stage, ACB are easier to handle (identical to tissue samples), while CTB are more challenging. Even if technical issues found in CTB processing are

similar to the ones encountered when dealing with routine histology of small biopsies, cells pellets are less cohesive than tissues and additional care and manual skills are required in tube extraction and embedding. However, with minimal training, a skilled histotechnician can obtain satisfactory results after few attempts. Two CTB were lost during processing phase. In both cases only a single tube was produced because of the low cellularity of the sample and the CTB was very short. One sample was lost during embedding while the other was over-sectioned. These losses were not related to specific sample features and that their occurrence was accidental. In those cases, a greater volume of fluid would have ensured a longer pellet (Marcos 2017) and would have allowed to prepare more tubes. This is advisable in every case to ensure that enough material for analysis is collected and that eventual technical accidents can be compensated.

Non-neoplastic non-haemorrhagic samples were not included, because this type of effusion is marginally involved in ancillary testing in routine practice. However, based on this experience and on data reported in literature (Marcos 2017, Marcos 2019) the two methods would have provided similar results, as long as poorly cellular samples are concentrated, and a high-density solution is used in CTB in absence of visible RBC.

In conclusion, both investigated fluid-to-solid conversion techniques able to provide sections of different types of effusion specimens for subsequent IHC studies. Cellular artifacts and background materials are occasionally present but the morphological and IHC interpretation is not compromised. CTB present some advantage in RBC rich samples providing higher cellularity and better separation of nucleated cells. However, they require little additional training of technical personnel in the processing phase. Considering these results, cell blocks are a useful tool for further characterisation of cells in canine and feline effusions. The choice of the method to be used should be based on specific specimen features (for example, haemorrhagic or not) and on the clinic and laboratory facilities.

2. ADVIA 120 CYTOGRAMS

2.1 INTRODUCTION

Automated analysis plays a pivotal role in diagnostic laboratories. It provides repeatable results and is less operator dependent, it reduces turnaround time and increases the overall efficiency of the laboratory. Automated cell counts of TNC and RBC are reliable if compared with manual counts. Conversely, automated differential counts have been shown as inaccurate and manual count on smears should be performed (Gorman 2009, Pinto de Cunha 2009, Brudvig 2015). However, different patterns of the cytograms of the automated analysers may represent specific cytologic features. For instance, the interpretation of Sysmex XT-2000iV cytograms has 60% concordance with the cytological diagnosis in canine and feline effusions (Pinto de Cunha 2009). In 2005, Bauer and Moritz suggested some interpretation keys for ADVIA 120 cytograms in effusions of dogs and cats. In this section the diagnostic performances of the cytograms patterns described by Bauer and Moritz in 2005 where evaluated in a retrospective study on canine effusions using the standard analysis as the gold standard.

2.2 MATERIALS AND METHODS

The cytology database of the Veterinary Clinical Pathology Laboratory of the University of Turin was searched for canine pleural, peritoneal, and pericardial effusions collected between January 2017 and December 2018. Cases with available matched cytology smears, ADVIA 120 cytograms and TP_{ref} were included.

Cytology

Cytological slides were reviewed by a senior cytologist, for each case one direct smear, one cytocentrifuged preparation, TP and automated WBC and RBC counts were provided. All slides were stained with May-Grunwald-Giemsa. Cytological diagnoses were grouped according the scheme reported in the data analysis section. No diagnostic modifiers were allowed, in doubtful cases the opinion of a second senior clinical pathologist was asked until reaching a consensus diagnosis.

ADVIA 120 automated blood analyser

ADVIA 120 provides a complete cell count and a five-population differential count which are optimized for canine peripheral blood. Results are displayed in scatter plot diagrams (cytograms). ADVIA 120 uses two separate channels for WBC – the peroxidase channel (Perox) and the Baso/lobularity channel (Baso). The peroxidase channel measures the intensity of the peroxidase reaction and the volume (size) of the cells. Cells are divided in seven regions (debris, lymphocytes, large unstained cells (LUC), monocytes, platelet aggregates, neutrophils, and eosinophils). In the Baso channel cells are treated with phthalic acid which strip the cells membranes (except humans' basophils) and the morphology of the nuclei is measured. Lobularity (side scatter) and volume (forward scatter) are then plotted, and

three regions are defined (mononuclear non-lysis resistant, polymorphonuclear non-lysis resistant and lysis resistant). Platelets are plotted in a separate cytogram displaying their volume and granularity.

The interpretation of the cytograms was performed by a PhD student with 3 years-experience in interpretation of ADVIA 120 cytograms and flow cytometry plots. For each case, TP_{ref}, and the complete ADVIA 120 output were provided. ADVIA 120 diagnoses were based on the interpretation keys previously described (Bauer and Moritz 2005) and summarized in (Tab.8). The diagnostic categories were the same use for the cytological evaluation. In doubtful cases the opinion of a second senior clinical pathologist was asked until reaching a consensus diagnosis.

Data analysis

With both methods effusions were classified in four groups neoplastic, haemorrhagic, transudates and exudates. Neoplastic effusions were further classified into three subgroups: lymphoma, malignant histiocytic, and non-haematopoietic (including epithelial and malignant mesothelial cells). Exudates were divided according to the prevalent inflammatory population in neutrophilic, macrophagic, mixed (neutrophils and macrophages equally represented) lymphocytic (including chylous effusions) and eosinophilic. The presence of bacteria and signs of degeneration was also recorded, these samples where classified as previously and further flagged as 'septic'. For the same reason chylous effusions, although commonly classified as modified transudates, were included in the group 'exudates with predominance of lymphocytes' because of similar features in terms of cell populations.

The diagnosis based on standard analysis (TP_{ref}, automated TNCC and RBCC, cytology) was used as gold standard, diagnostic performances were calculated for neoplastic, haemorrhagic, transudates, exudates, and septic effusions over all cases. For these categories, both complete (group and subgroup) or partial (only group) agreement were considered as a true positive result. The performances of the subgroups of neoplastic and exudates were calculated within their groups. In these cases, only a complete agreement at both group and subgroup level was considered as a true positive result. 2x2 contingency tables were prepared and diagnostic accuracy indexes were calculated including accuracy (Ac), sensitivity (Se), specificity (Sp). Diagnostic indexes were interpreted as low (<69%), moderate (70-79%), high (80-89%), very high (>90%).

Table 8. ADVIA 120 cytogram features for each diagnostic group (Bauer and Moritz 2005)

	Peroxidase	**Baso/Lobularity**	**Platelets**	**Notes**
Lymphoma	Lymphocyte population extending in the LUC region depicting an abnormal cluster.	Large population of mononuclear cells extending into the blast/baso region ('nose').		Hypercellular
Malignant histiocytosis	Large cell population located in monocytes' and LUC regions clearly separated from small lymphocytes (if present).	Predominance of mononuclear to slightly polymorphonuclear cells extending into the region of lysis resistant cells.		Hypercellular
Epithelial and mesothelial cells	LUC not or poorly increased.	Non-lysis-resistant blast populations in the mononuclear region (which is not evident in the LUC's region)		Variable cellularity
Inflammatory	Hematopoietic populations with cellular distribution pattern similar to peripheral blood	Hematopoietic populations with cellular distribution pattern similar to peripheral blood		The prevalence of one population determined the subtype of inflammation
Haemorrhagic	WBC as blood, slight increase of LUC	non-lysis-resistant blast populations in the mononuclear region (reactive mesothelial cells)	Low PLT then peripheral blood	High RBC content (> 0.5-1x10^6/uL)
Transudate	Cells spread diffusely over all areas	non-lysis-resistant blast populations in the mononuclear region (reactive mesothelial cells)		WBC <5x10^3/uL, TP variable (protein-poor/rich transudate)
Septic	Distinct populations in neutrophil and monocyte regions, with an abnormal distribution. Large cluster extending from debris and PLT clumps regions into the neutrophilic and monocytic areas.		Increased in the lower left area	

2.3 RESULTS

Patient's demography

Two-hundred and twenty-four effusion samples were submitted for full fluid analysis in two years. Thirty-six cases were excluded. In particular, in 26 samples the analysis was not performed the same day of collection, in 4 cases ADVIA 120 analysis was not performed due insufficient sample (N=2) or for the presence of floccules (risk of clotting the instrument, N=2), cytological slides were not available in 3 cases, and the value of total proteins was not available in one case. Therefore, 188 effusions of 179 different patients with matched cytological slides, ADVIA 120 cytograms, and TP_{ref} were included. Samples were collected from pleural (N=79), pericardial (N=29) and peritoneal (N=80) cavities. Patients sex was not available in 6 cases, while the remaining patients were 43 females, 84 males, 44 spayed females and 11 castrated males. The age was available in 175 patients (average 8.97 years; range 10 months – 16 years). Cross breed dogs were the most represented species (N=69), then Labrador Retrievers and German Shepherds (15 each), followed by Golden Retrievers (9), Boxer, Cane Corso, Rottweiler (6 each), English bulldog, Doberman Pinscher (5 each), Border Collie, Dogue de Bordeaux, Australian Shepard, Yorkshire Terrier (4 each), Chihuahua (3), Dachshund, Pug, Cavalier King Charles Spaniel, Jack Russel Terrier, Greyhound, English Setter (2 each), American Staffordshire Terrier, Boston Terrier, Bernese Mountain Dog, Deutsch Kurzhaar, Bull Mastiff, Bull Terrier, Dogo Argentino, Hovawart, Pekingese dog, St. Bernard Dog, Riesenschnauzer, Volpino Italiano, West Highland White Terrier (1 each). The breed of 4 patients was not specified in the records.

Neoplastic samples

ADVIA 120 cytogram interpretation identified 64/72 (88.8%) neoplastic cases, 61/64 (95.3%) with complete agreement and 3/64 (4.7%) with partial agreement. Sensitivity and specificity for identification of neoplastic effusions were 88.9% and 98.3% respectively. In particular, lymphoma (Fig.3A) related effusions were correctly identified 16/18 cases (Se 88.9%, Sp 98.1%), the remaining two cases were interpreted as exudate with prevalence of lymphocytes. Over 6 effusions caused by malignant histiocytosis (Fig.3B), 4 were correctly diagnosed by ADVIA 120 cytogram interpretation (Se 66.7%, Sp 100%), while 2/6 (33.3%) were diagnosed as malignant NH. 41/48 malignant NH (Fig.4A-B) effusions were correctly identified (Se 85.4%, Sp 91.7%), while the remaining were diagnosed as neutrophilic exudates (N=4), transudates (N=3) or lymphoma (N=1).

Non-neoplastic samples

Among non neoplastic cases, ADVIA 120 cytogram interpretation correctly identified all haemorrhagic effusions (N=30) (Fig.4C), all transudates (N=11) and 66/75 exudates. Among exudates, 53/66 (80.3%) with complete agreement and 13/66 (19.7%) with partial agreement. Sensitivity and specificity

were 100% and 100% for haemorrhagic effusions, 100% and 94.9% for transudates, 88% and 95.6% for exudates regardless the subgroup.

Regarding the subtypes of exudates, eosinophilic inflammation was correctly identified in 4/4 cases (100%) (Se 100%, Sp 100%). Six out of 7 (85.7%) lymphocytic effusion were correctly identified (Se 85.7%, Sp 98.5%) while 1 sample was diagnosed as lymphoma. ADVIA 120 failed to recognize all macrophagic effusion (N=4) which were diagnosed as transudate (N=1), mixed (N=1) or neutrophilic (N=2). Mixed inflammation was identified in 4/15 cases (26.5%) (Se 26.7%, Sp 95%); the remaining cases were incorrectly diagnosed as neutrophilic (N=6), transudates (N=4), and lymphocytic (N=1). Finally, 39/45 (86.6%) neutrophilic exudates were correctly diagnosed (Se 86.7%, Sp 73.3%) while the remaining were defined as transudate (N=2), mixed (N=2), macrophagic (N=1), and neoplastic NH (N=1).

Lastly, in 13 cases free and phagocytized bacteria were observed in cytology (Fig.3C). ADVIA 120 correctly identified septic exudates in 6/13 cases (46.5%) with no false positive results (Se 46.2%, Sp 100%). In particular, false negative cases were interpreted by ADVIA 120 cytograms as transudates (N=2), purulent non-septic (N=4) and neoplastic non-haemopoietic (N=1). Cytology slides were reviewed and revealed in all false negative cases the presence of rare to low number of bacteria and slight to mild signs of degeneration in neutrophils, while ADVIA 120 cytograms had more defined neutrophils populations, less debris, less events in PLT clumps area in peroxidase cytogram and less PLT in the PLT cytogram when compared to the model cytogram and other septic cases.

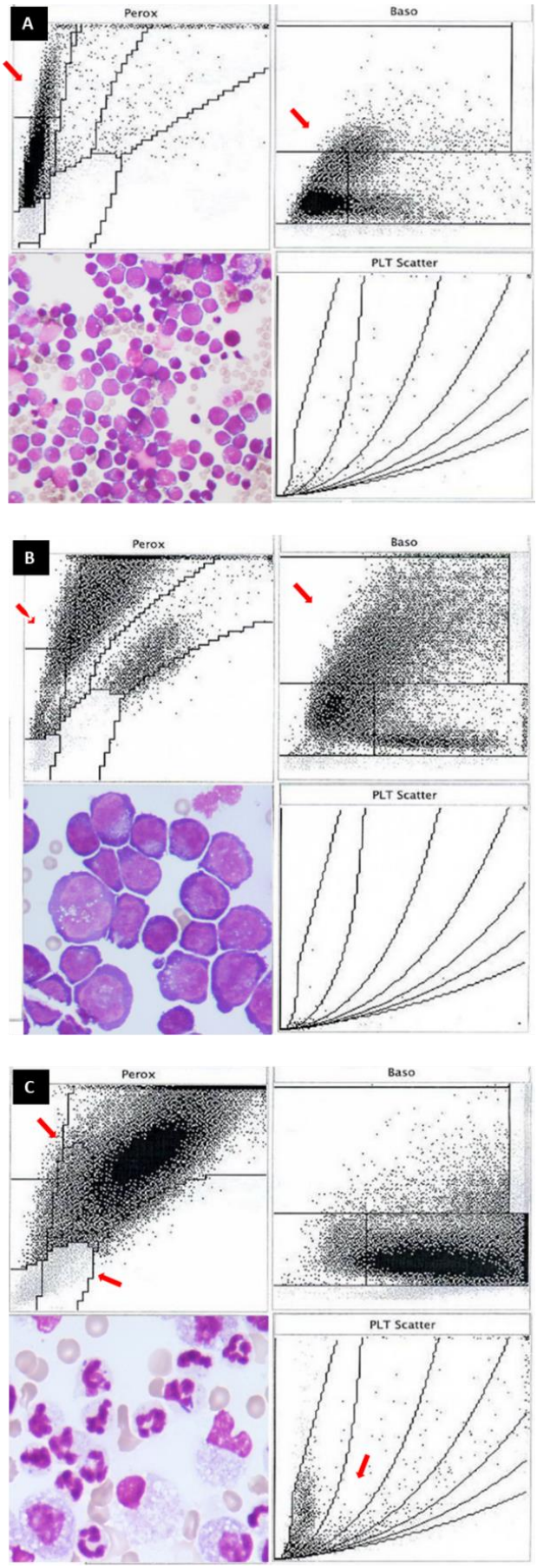

Figure 3. ADVIA 120 cytograms and matched cytology. From top left, clockwise: Perox cytogram, Baso/Lobularity cytogram, platelets cytogram, MGG cytology.

A. Dog, peritoneal effusion, lymphoma. In Perox, neoplastic cells represent almost the only present population, they mainly occupy the lymphocytes area, extending to the LUC. In Baso/lobularity cells are in the mononuclear area with partial lysis resistance. PLT cytogram is unremarkable.

B. Dog, pleural effusion, malignant histiocytosis. In Perox, very large cells cluster across monocytes, LUC, and lymphocytes areas, with a visible separation with normal small lymphocytes. In Baso/Lobularity, lysis resistance is more evident than in lymphomas. PLT cytogram is unremarkable.

C. Dog, peritoneal effusion, septic purulent effusion. A massive, poorly defined cluster of neutrophils extending towards PLT clumps and debris areas is evident in Perox. Baso/Lobularity cytogram is unremarkable. Events are evident in PLT cytogram, probably representing cellular debris.

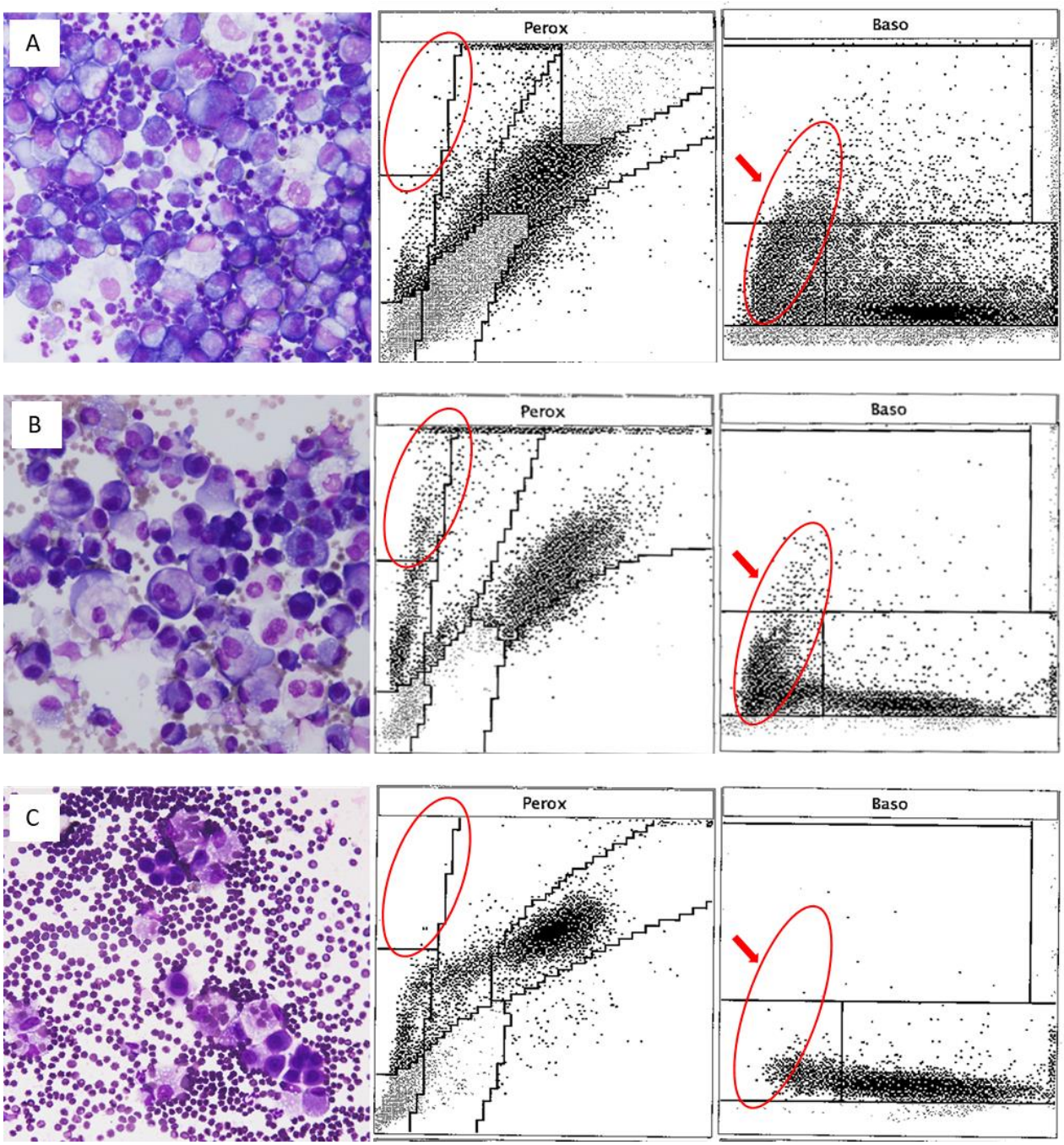

Figure 4. ADVIA 120 cytograms and matched cytology. From left to right, cytology (MGG), Peroxidase cytogram, Baso/Lobularity cytogram. PLT cytogram unremarkable in all cases, not shown. A-B. Dogs, pleural effusions with neoplastic epithelial cells, presence of non-lysis resistant mononuclear cells in Baso/Lobularity, note the absence or low number of events in LUC area of Perox. C. Dog, pericardial effusion with reactive mesothelial cells (haemorrhagic). WBC cytograms similar to peripheral blood, no populations are present in expected gates for mesothelial cells.

2.4 DISCUSSION AND CONCLUSION

Automated blood analysers are reliable instruments for RBCC and TNCC in effusion, (Gorman 2009, Pinto de Cunha 2009, Brudvig 2015). However, they are not reliable for differential counts and only a moderate concordance (60%) between Sysmex XT-2000iV cytograms and cytology was found (Pinto de Cunha 2009). Cytogram patterns for effusions have been described for ADVIA 120 (Bauer 2005). In this part of the study these interpretation keys were retrospectively applied to determine the diagnostic performances of ADVIA 120 cytograms.

ADVIA 120 diagnostic performances in identification of neoplastic subtypes had very high specificity (98.3%) and variable sensitivity depending on the subtype (66.7%-89.5%).

In particular, lymphoma associated effusions showed the best performances, these samples tended to be hypercellular and the presence of inflammatory populations was minimal, further in the peroxidase cytogram the population was narrowed and condensed (monomorphism), rising from the lymphocytes region and extending to the LUC area (medium-large size without peroxidase activity). In the baso/lobularity cytogram the majority of the cells were condensed in the mononuclear area extending into the lysis resistant region in a comet tail shape (nose), suggesting that a small part of the population is variably resistance to lysis.

When comparing the cytograms described for neoplastic medium-large lymphocytes with malignant histiocytic cell, the latter appeared less clustered in both perox and baso/lobularity cytograms. In perox channel, these cells were clearly separated from the lymphocytes (larger size) and had variable, mild to moderate perox activity occupying an area covering the LUCs, monocytes and partially neutrophils regions. In the Baso cytogram these cells had a less compact distribution, were shifted towards the polymorphonuclear region and variably lysis resistant. In the two false negative cases, these features where less prominent because of a lower relative number of neoplastic cells in the fluid leading to a misinterpretation of the cytograms.

Cytograms for epithelial and mesothelial cells had less specific and constant features than the ones of hematopoietic neoplasms. The presence of epithelial and mesothelial cells in the fluid should be suspected in presence of a non-lysis resistant population in the mononuclear area (baso/lobularity) extending parallel to the Y axis in the leftmost part of the cytogram and the absence of a population in the LUC of the Perox cytogram (Bauer and Moritz 2005). This latter feature lead to a higher discrepancy in the WBC count performed on the Perox and Baso/lobularity channels. In this series, these patterns were more prominent but more variable than previously described (Bauer and Moritz 2005) (Fig.4A-B). This likely reflects the high variability of presentation of neoplastic non-hematopoietic cells among different samples.

According to these interpretation keys, reactive mesothelial cells have similar pattern of neoplastic epithelial and mesothelial cells and are therefore not distinguishable. However, in this series of cases only a few cases where only reactive mesothelial cells were present (e.g., virtually all transudates, inflammatory, haemorrhagic effusions) showed the specific pattern previously described (Fig.4C). This is probably due to the much lower absolute (e.g., transudates) or relative count of reactive mesothelial cells if compared to the inflammatory/blood derived population (e.g., inflammatory and haemorrhagic effusions).

As a consequence, low numbers of malignant epithelial and mesothelial cells may result in intermediate and less prominent pattern leading to a false negative interpretation. Similarly, although less frequent in this case series, non neoplastic effusion with high numbers reactive mesothelial cells and low number of inflammatory cells can be misdiagnosed as neoplastic.

Diagnostic performances for haemorrhagic effusions were straightforward. This result was expected as the diagnosis of these effusions is mostly based on the RBC cell count whereas cytology and the cytograms mainly rule out other effusion types and support the diagnosis. Notably, ADVIA 120 analysis overestimated transudates, this happened when a combination of low TP, low cellularity and mixed inflammatory cells acted as confounding factors resulting in a low specificity.

Overall, ADVIA 120 diagnosis of inflammatory effusions showed moderate to good performances, interestingly, this varied according to the inflammatory subtype and it is probably due to specific features of each cell type in the cytograms. In particular, eosinophils and lymphocytes regions are highly specific and only few other cell types might be present in the same area. Only one case with reactive lymphocytes was wrongly interpreted as lymphoma. Conversely macrophages, being highly variable in terms of size, complexity, and peroxidase activity, do not occupy a specific area on the cytogram and are variably spread among LUC, monocytes and neutrophils regions. Further they do not cluster in a definite compact population. All these factors contribute to a more difficult identification of this cell type leading to low performances for both macrophagic and mixed exudates. Lastly, neutrophilic exudates had the worse overall accuracy. As neutrophils are present in almost all effusions, when other patterns are absent or not evident neutrophils are likely considered the main population leading to a lower sensitivity and specificity.

Septic effusions are characterised by neat prevalence of neutrophilic inflammation, generally with severe degenerative features (pyknosis and karyorrhexis) and the presence of bacteria which may eb seen both free and engulfed by neutrophils. According to Bauer and Moritz 2005, in ADVIA 120 cytograms these features result in an increased density of the neutrophils population in the peroxidase cytogram with less defined borders, and the tendency to extend in the monocyte and platelet clumps area. Furthermore, debris are evident in Perox and may be seen also in the PLT cytogram in its lower left part. In this subset of cases, ADVIA 120 cytogram interpretation was highly specific but poorly

sensitive; more than 50% of cytologically diagnosed septic effusions did no display the expected cytogram features. Interestingly the cytological slides revision revealed a milder degeneration of neutrophils and lower numbers of bacteria. Therefore, as ADVIA 120 cytogram diagnosis of septic effusion rely on features determined by the presence of degenerated cells, when this phenomenon is less evident the method fails to detect septic effusion. For this reason, other causes of marked neutrophils degeneration and debris (i.e. old sample, incorrect storage) might produce a false positive result. Being highly specific ADVIA 120 cytograms of septic samples anticipate the cytological diagnosis when specific features are present, however in the absence of these features this differential diagnosis should not be ruled out.

In conclusion, the automated analysis with ADVIA 120 provides useful data for the diagnosis and classification of canine cavitary effusions. Apart from red blood cells and nucleated cells counts, cytograms interpretation also provide useful information at no additional costs. Cytograms are highly specific for particular features and are able to anticipate and support the cytological diagnosis. In particular, there are subsets where specific patterns are almost unequivocally diagnostic (e.g., large cells in lymphomas, malignant histiocytosis and non-hematopoietic cells). On the side, in case of inflammatory effusions, diagnostic features highly depended on the prevalent inflammatory cell type (better for lymphocytes and eosinophils, worse for macrophages), on the presence of confounding factors (e.g., presence of high numbers of reactive mesothelial cells) and on the presence of specific case dependent features (e.g., degree of degeneration in septic effusions). Finally, in case of haemorrhagic effusions and transudates cytograms evaluation can be used to confirm these differentials based on cell counts and total proteins, and to rule out the presence of other atypical populations. However, it is important to remind that cytogram are specific for particular morphologic features of the cells, thus, when these features are not present or are not prominent the accuracy is markedly reduced. For this reason, cytogram interpretation should not be considered a replacement for cytological evaluation but a tool to anticipate, consolidate and accelerate the cytological evaluation reducing the turnaround time for the diagnosis and the selection of the appropriate ancillary technique.

3. FLOW CYTOMETRY

3.1 INTRODUCTION

Flow cytometry (FC) is an advanced technique used to measure physical and fluorescent properties of the analysed particles. The combination of physical and fluorescent data allows the characterisation of multiple population within the same sample. In diagnostic veterinary clinical pathology, FC is routinely used to refine the cytological diagnosis of lymphomas and leukaemias.

FC is a semiautomated method that provides quantitative measurements, it is able to analyse large numbers of particles in a relatively short time. Further, it allows multicolour panels which make the test economically affordable considering the number of antibodies that can be used at the same time.

Apart from hematopoietic disorders, its diagnostic usefulness has been proved in humane medicine also for NH cells in effusion, whereas this field has not been investigated in veterinary medicine.

This study is aimed to develop a flow cytometric staining and gating strategy able to identify and characterise NH cells in canine effusion. Additionally, staining features of FC and IHC on cell blocks are analysed to provide interpretation keys for the different encountered patterns.

3.2 MATERIALS AND METHODS

Canine cavitary effusions were collected from dogs attended at Veterinary Teaching Hospital of the University of Turin (Grugliasco, IT). Dogs were privately owned and underwent sampling for diagnostic purposes with the informed consent of the owners.

Samples were collected in EDTA and plain tubes and processed according to routine effusion analysis including gross aspect, total cell count with an automated hematological analyser (ADVIA 120), refractometric total proteins, specific gravity, and cytological preparations.

Samples with cytological evidence of atypical cells suspicious for NH origin were included. Samples with abundant reactive mesothelial cells were also included as controls. A minimum residual volume of fluid of 4 ml in K3EDTA was needed to further process the samples. Within 24 hours from collection, all samples were processed for FC and cell blocks were prepared up to fixation. To consolidate the cytological interpretation of NH origin of the cells additional, pathological, clinical, imaging and follow-up data were collected when available.

Flow cytometry

To define samples' quality and assess autofluorescence levels, 20uL of unstained sample were diluted (1:10) with an RBC lysis solution to remove RBC from the analysis. The ammonium chloride-based lysis

buffer was incubated for 5 minutes at RT in the dark then acquired. Cell vitality was evaluated incubating cells with propidium iodide (PI) for 10' at RT in the dark and directly acquired.

Surface and Cytoplasmic Staining

$5x10^5$ cells were placed in each polypropylene tube, RBC were removed adding lysis buffer. After centrifugation, the cell pellet was resuspended in RPMI-1640 containing 5% foetal calf serum (FCS) and incubated for 15' at 4°C to block non-specific binding, washed and resuspended with 40uL of PBS.

A screening panel of surface antibodies (Tab.9) was run to identify the different populations. Cells were incubated with previously titrated monoclonal antibodies for 20' at 4°C in the dark, washed twice with PBS and immediately acquired. Unstained cells of the same sample were included in each run as negative control. Fluorescence minus one (FMO) controls were run in pilot cases to address spill over-induced background and set proper compensations.

Intracellular staining was performed with a 2-color approach using CD11b to stratify different populations (see later). Cells were firstly labelled with surface CD11b PE-Cy5 as described before, then processed for cytoplasmic staining with a commercial intracellular staining kit (eBioscience™ Intracellular Fixation & Permeabilization Buffer Set, ThermoFisher). Briefly, cell pellets were resuspended in paraformaldehyde-based fixation buffer and incubated for 10' at 4°C, washed once with PBS and twice with saponin-based permeabilization buffer. 40uL of permeabilization buffer and the monoclonal antibody against intracellular antigens (Tab.9) were added and incubated for 30' at 4°C, washed twice with permeabilization solution and immediately acquired at the cytometer. For indirect labelling, after the second wash with permeabilization solutions cells were additionally incubated for 20' at 4°C with FITC-conjugated secondary antibody, then washed with permeabilization buffer and acquired.

Unstained cells, isotype control or omission of primary antibody for indirect staining, were included in each run, FMO controls were run in pilot. A minimum of 40.000 total events were acquired for each tube with a 2-laser- 4-channels flow cytometer (Accuri C6, Becton Dickinson). Forward and side scatter parameters were defined in linear amplification, while fluorescence parameters (FL1, FL2, FL3, FL4) were defined in logarithmic amplification mode, the threshold was based on FSC as a primary parameter to excluding small debris.

Table 9. Details of antibodies used in flow cytometry

Antibody	Conjugation	Clone	Source	Host	Reactivity	Target
CD44	FITC	IM7	Thermo-Fisher	Rat	Mouse	Pancellular
CD45	FITC	YKIX716.13	Bio-Rad	Rat	Dog	Panleukocyte
CD18	AF647	CA1.4E9	Bio-Rad	Mouse	Dog	Panleukocyte
CD11b	PE/Cy5	M1/70	Abcam	Rat	Mouse	Granulocytes, monocytes
MHC-II	FITC	YKIX334.2	Bio-Rad	Rat	Dog	Lymphoid, monocytes
CD14	FITC	TUK4	Bio-Rad	Mouse	Human	Monocytes
CD5	FITC	YKIX322.3	Bio-Rad	Rat	Dog	T-cell
CD5	AF647	YKIX322.3	Bio-Rad	Rat	Dog	T-cell
CD21	AF647	CA2.ID6	Bio-Rad	Mouse	Dog	B-cell
IgG1a	AF488		NovusBio	Mouse	Human	Isotype
Pan-cytokeratin	AF488	CK AE1/AE3	NovusBio	Mouse	Human	Epithelial, mesothelial*
Vimentin	AF488	V9	NovusBio	Mouse	Human	Mesenchymal, mesothelial, leukocytes*
Desmin	unconjugated	DER-II	Novocastra	Mouse	Human	Mesothelial, muscles*
IgG	FITC		Bio-Rad	Rat	Mouse	Secondary antibody

Plots Analysis

Analyses were performed with CFlow Plus software (Becton Dickinson). Intact single cells and target cells (see later) were plotted in FSC-A/FL-x-A for each channel to evaluate the autofluorescence and set cursors. The positive gate was depicted to include less than 1% of the events referring to negative controls (unstained cell of the same autofluorescence or isotype control). Morphological and fluorescence features were collected recording median values of FSC-A, SSC-A and FL1-A (autofluorescence) in unstained control tubes.

For NH cells characterisation, immunoreaction to surface and cytoplasmic antigens were described. Particularly, percentage of positive target cells was recorded. Immunoreaction was defined positive only when at least 20% of the target population had an unequivocal separation from negative control. Positive signal intensity was defined as bright or low and median fluorescence intensity (MFI) of the target population was recorded in FL-1. The median fluorescence intensity index (iMFI) was calculated as (Adivani 2008):

$$iMFI_{target} = \frac{(MFI_{\text{FL-1 } Stained})_{target}}{(MFI_{\text{FL-1 } Isotype})_{target}}$$

Magnetic cell sorting

Magnetic cell separation was used to verify the ability of CD11b to separate NH-cell from other populations in the samples. The experiment was performed on a fresh sample of pleural effusion with cytologically and histologically confirmed epithelial cells. Sample populations were firstly studied by FC through multicolour surface staining, then cells were labelled with unconjugated CD11b and incubated with the secondary MicroBeads conjugated antibody (Anti-Mouse IgG1 Microbeads, Miltenyi Biotec, Auburn, CA). The cell suspension was loaded onto a separation column (MS MACS column, Miltenyi Biotec, Auburn, CA) exposed to a magnetic field (MACS Separator, Miltenyi Biotec, Auburn, CA) allowing the microbeads to adhere to the column wall. Column was washed and the negative selected fraction, composed by unlabelled cells run through the column was collected. The column was then removed from the magnetic field the retained cells were eluted as the positively selected cell fraction. An aliquot of the collected fractions was spun on a slide and stained with MGG for morphological assessment while the remaining part was labelled with the secondary FITC conjugated antibody (anti-mouse IgG1 FITC) and acquired at the cytometer. The degree of purity was determined as the percentage of CD11b negative and positive events in the negative and positive selected fractions, respectively.

Immunohistochemistry

IHC for cytokeratin, vimentin and desmin was performed for all the samples on formalin fixed paraffin embedded cell blocks. Four micrometres sections were cut and placed on Tomo® IHC adhesive glass slides (Matsunami glass Ltd.), dried in convection oven at 50°C for 30 minutes. IHC were performed in one session with an automated immunostainer (BenchMark XT processor, Ventana Medical Systems, Tucson, AZ). Sections were deparaffinized with xylene and rehydrated with ethanol. Endogenous peroxidase activity was inhibited with a peroxide hydrogen 3% solution and heat induced antigen retrieval was performed. Details of primary antibodies used are listed in Tab.10, incubation was performed at 37°C for 30 minutes for all antibodies. The Ventana ultraview universal DAB Detection kit (an indirect, biotin-free system for detecting mouse IgG primary antibodies) was used for all samples. Histological section of canine intestine, liver, pancreas, spleen, and lymph node were used as controls.

Table 10. Details of antibodies used in immunohistochemistry on cell blocks

Antibody	**Clone**	**Source**	**Host**	**Reactivity**	**Dilution**
Cytokeratin	CK AE1 AE3	NovusBiologicals	Mouse	Human	1:200
Vimentin	V9	Ventana	Mouse	Human	Prediluted
Desmin	DER-II	Ventana	Mouse	Human	Prediluted

IHC interpretation was performed reviewing MGG cytological preparation and HE stained cell blocks to ensure a proper identification of NH-cells and assess the immunoreaction. Immunohistochemical staining was semi-quantitatively scored based on both intensity and proportion of cells stained using a modified method as proposed by Hilary in 2009 (Tab.11). Staining patterns were also recorded.

Table 11. Immunohistochemical semi-quantitative scoring method adapted from an image analysis protocol (http://www.ihcworld.com/ihc_scoring.htm)*

Score	**0**	**1+**	**2+**	**3+**	**4+**
Positive cells (%)	<10	10-25	25-50	50-75	>75
Intensity	No staining	Weak stain	Moderate stain	Strong stain	-

* Total score= positive cell X intensity; maximum = 12

3.3 RESULTS

Twenty-four samples from the pleural (N=11), peritoneal (N=6) and pericardial (N=7) cavities were included. Based on available clinical-pathological data cases were grouped in reactive mesothelial cells (N=11), epithelial (N=7), mesenchymal (N=1), putative neoplastic mesothelial cells (N=5).

Due to the low number of cases in each group, statistical analyses were not performed. Data were descriptively reported, and tendencies analysed. Numerical data were expressed as median values and ranges in brackets.

Flow Cytometric Gating strategy

Events were firstly plotted for size and granularity (FSC-A/SSC-A), a wide gate was depicted including only evens with SSC and FSC higher than normal canine lymphocytes to exclude cell debris (Fig. 5A). Single cells were selected (FSC-A/FSC-H) (Fig. 5B-C) and plotted with the propidium iodide (FSC-A/PI-A) to exclude non intact cells (Fig. 5D). Viable cells were backgated for the morphological evaluation (FSC-A/SSC-A) of the populations and a restricted gate of analysis including only single, live, and intact cells was depicted (Fig. 5E-F).

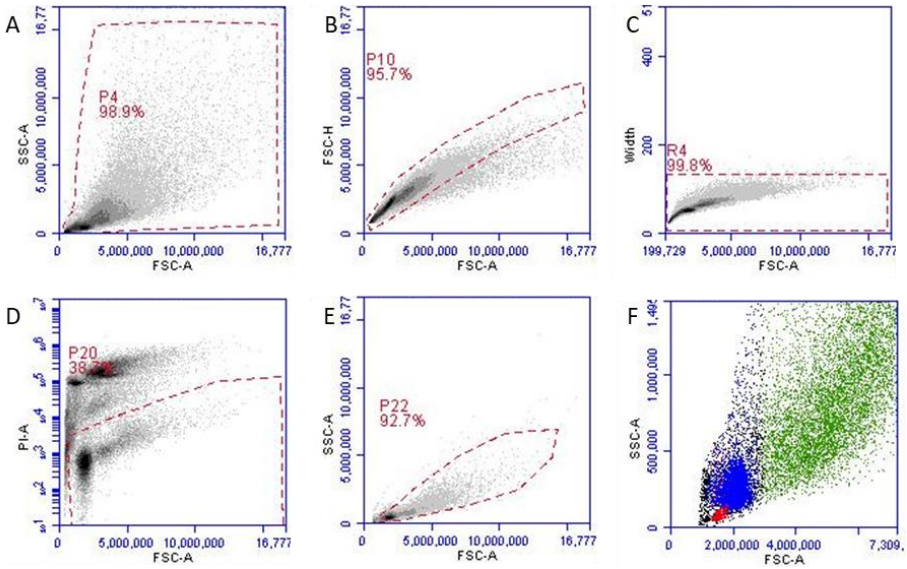

Figure 5. Gating strategy. Dog, pleural effusion. A, wide gate excluding only events smaller than normal canine lymphocytes. B-C, singllets selection. D, selection of living cells. E-F, gate of analysis.

Flow Cytometric Identification of Non-Hematopoietic Cells

In the gate of analysis, the combination of morphological scatters and surface markers allowed the identification and isolation of three main hematopoietic CD44+CD45+CD18+ populations: lymphoid cells (MHC-II+, CD5+/-, CD21+/-), granulocytes (CD11b+) and monocytes/macrophages (CD11b+, MHC-II+, CD14 var).

Additionally, a NH population CD44+CD45- (target population) was recognized. The target population had a high median FS (6615 $x10^3$, range 3586-11777) and highly variable median SS (1163 $x10^3$, range 372-6840). Autofluorescence in FL-1 (4992, range 1764-31141) was higher than normal lymphocytes and neutrophils and similar to the one of monocytes/macrophages CD44+CD45- events were consistently large and negative to CD11b, thus by plotting FS and CD11b the main populations where easily identifiable (Fig. 6). To further confirm the ability of CD11b to isolate NH cells magnetic cell sorting was performed.

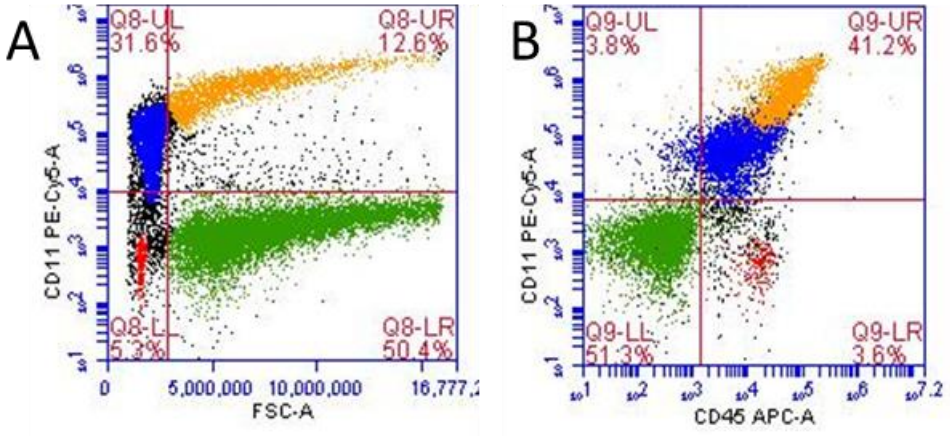

Size	CD11b	CD45	Population	Color
Small	Negative	Positive	Lymphocytes	Red
Medium-small	Positive	Positive	Neutrophils/Monocytes	Blue
Large	Positive	Positive	Macrophages	Yellow
Large	Negative	Negative	Putative NH cells	Green

Figure 6. Dog, pleural effusion. A, CD11b PE-Cy5 x FSC, four populations are isolated (see details in table) B. CD11b PE-Cy5 and CD45 APC, the only CD45 negative population is represented by large CD11b negative events.

Magnetic cell sorting

The CD11b positive selected fraction had a purity of 93.3% and was mainly composed by neutrophils and macrophages. The CD11b negative selected fraction had a purity of 87.1% and the cytological evaluation confirmed that was composed mainly by small lymphocytes and NH cells and rare neutrophils. Further, thanks to FS properties, the small (lymphocytes) and the large (NH cells) CD11b- populations were easily recognizable in all the samples (Fig.7).

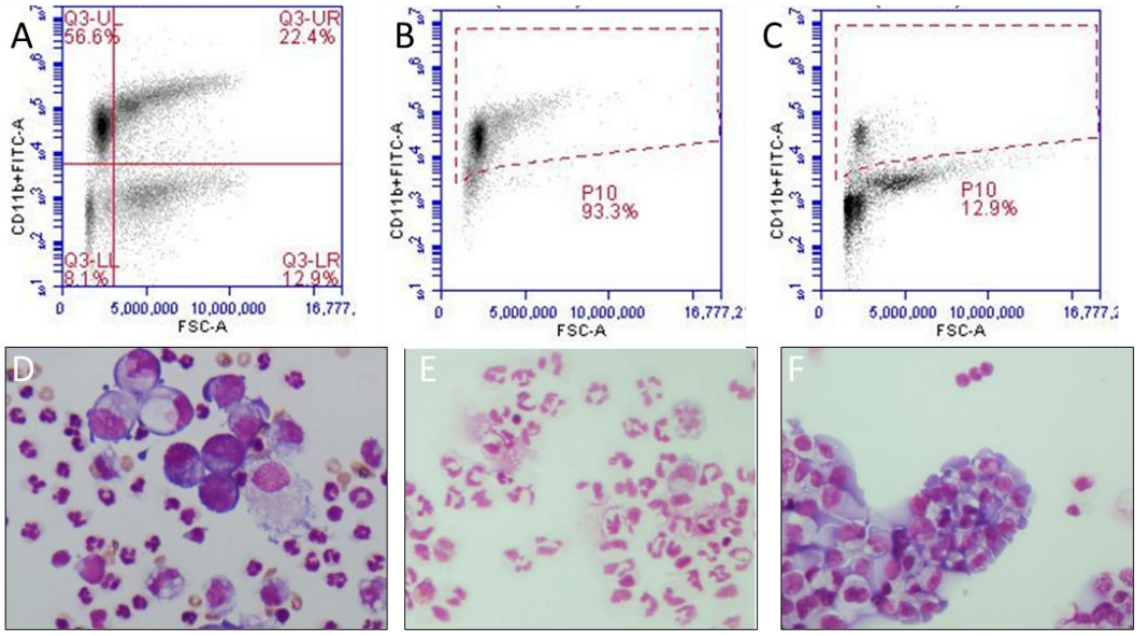

Figure 7. Magnetic cells sorting. Pleural effusion of a dog with lung carcinoma metastatic to the pleura. A CD11b stainign before magnetic cell sorting, note two positive popualtions in different quadrants:medium CD11b+(neutrophyls), large CD11b+ (macrophages), small CD11b- (lymphocytes), large CD11b- (putative neopalstic cells). D. Cytological prepration of the same sample, the four mentioned populations are evident, May-Grunwald Giemsa, 40x. B, E, positive selected fraction with magnetic cell sorting. C, F, negative selected fraction with magnetic cell sorting.

Non-hematopoietic cells characterisation

Overall, FC and IHC agreement in markers interpretation (positive or negative) was 100% (24/24) for CK and DES while it was 79.1% (19/24) for VIM. Particularly, 5/5 discordant cases were interpreted as VIM positive in IHC and negative in FC. NH cell in discordant cases were reactive mesothelial cells (2/5) and epithelial cells (3/5).

Among positive cases a bright signal in FC was related to a strong and diffuse cytoplasmic reaction in IHC. Whereas a low signal in FC corresponded to a patchy pattern an/or a low-moderate intensity in IHC.

Epithelial (n=7)

In IHC, CK reaction was diffuse, strong (score 3), and observed in >75% on NH cells in all cases (IHC score 12/12). In FC, CK was positive in all cases and the proportion of positive events was 91.2% (88.3-99.1%). Signal was bright in 6/7 cases (iMFI 14.6, 11-45.2) and low in 1/7 cases (iMFI 3.9). (Fig. 8)

In IHC, VIM was positive in 6/7 cases with a patchy (4/6) or mixed (2/6) cytoplasmic pattern. Staining intensity was moderate (score 2) in all cases but one (score 3). The number of positive cells in each sample was variable 10-25% (2/6), 25-50% (2/6), 50-75% (1/6) and >75% (1/6). Final IHC score was 5 (2-12). In FC, VIM was positive in 3/7 cases and negative in 4/7 cases. In positive cases the proportion of positive events was 59% (34.2-72.6) and the intensity of the signal was low (iMFI 3.4, 2.2-4.5). In cases interpreted as negative the proportion of observed positive events was 7.4% (1.3-14.1). Cases interpreted as positive low in FC had a mixed (2/3) or diffused (1/3) cytoplasmic pattern and had the highest IHC scores for VIM in the epithelial group (4, 6 and 12). In discordant cases (negative in FC and positive in IHC, 3/6) IHC staining pattern was patchy in all cases and IHC scores were among the lowest (2, 2 and 4). (Fig 8-9)

In both IHC and FC desmin was negative in all cases. In IHC, few (<10%) scattered cells with diffuse strong reaction were present in all cases. Similarly, in FC rare to occasionally moderate numbers of DES positive events (1.1, 0.7-19.3%) were observed among NH cells. (Fig. 8)

Mesenchymal (n=1)

Only one case with neoplastic mesenchymal cells was collected. FC and IHC were concordant in the interpretation of all the three markers with CK-VIM+DES- profile.

In IHC, VIM expression was strong, diffuse, and present in all NH cells. Similarly, in FC the proportion of positive cells was 99.3% and the iMFI was 57.7. (Fig. 8)

Reactive Mesothelial Cells (n=11)

The profile CK+VIM+DES+ was observed in 11/11 cases in IHC and in 8/11 cases in FC. In two cases VIM was negative in FC.

In IHC, CK reaction was diffuse, strong (score 3) and observed in >75% on NH cells in the majority of the cases (10/11). Final average IHC score was 11.5/12 (6-12). In FC, CK was positive bright in all cases (iMFI 21.4, 6.9-49.7). The proportion of positive NH events was 91.2% (50.3-98.6). (Fig. 8)

Similarly, VIM reaction was positive in all cases mainly with a diffuse distribution (9/11) and strong intensity (8/11) although the proportion of positive cells was more variable if compared with CK (>75% in 4/11 cases, 50-75% in 5/11 cases and 25-50% in 2/11 cases). Final IHC score was 8.8/12 (4-12). In FC, VIM was interpreted as positive in 9/11 cases, the proportion of positive NH events was 62.3% (32.2-96.3). Among positive cases 5/9 had bright intensity (iMFI 11.9, 7.4-18) and 4/9 had low intensity (iMFI 2.48, 2.11-3.48). Two cases were interpreted as negative (less than 4% of positive events). FC bright intensity cases had diffused distribution and a high IHC score (11.4/12) while cases defined as low intensity in FC had lower IHC scores (7/12). Two cases had discordant VIM interpretation: in one case the IHC staining was strong and diffuse but only in 25-50% of the cells, while in the other case it was moderate, with a patchy distribution and observed in 50-75% of the cells. Both cases had an IHC score of (6/12). (Fig. 8)

In IHC, DES reaction was diffuse and strong (score 3) in the majority of the cases (8/11). In 3/11 cases the cytoplasmic reaction had a multifocal cytoplasmic distribution. NH cells with a positive reaction to DES were >75% (6/11) or between 50-75% (5/11). Final IHC score was 9.8/12 (6-12). In signal was bright in 9/11 cases (iMFI 7.23, 2.7-18.8) and low in 2/11 cases (iMFI 1.92, 1.96). This last two cases showed a focal distribution with a moderate staining intensity (score2) in 50-75% of the cells (IHC score 6/12). (Fig. 8)

Putative Neoplastic Mesothelial Cells (n=5)

All the cases included in this group had the following features: bicavitary effusion, no evidence of primary tumour or history of neoplastic diseases, highly aggressive behaviour, cytological features suggestive of mesothelial origin. Histopathology was not available in four cases, in one case pleural biopsies were performed but did not yielded diagnostic material.

The profile CK+VIM+DES- was observed in 5/5 cases in both FC and IHC.

In IHC, CK reaction was diffuse and present in >75% on NH cells in 4/5 cases. In one case it had a granular pattern in 50-75% of the cells. Staining intensity was strong (3/5) or moderate (2/5). Final IHC score was 10/12 (6-12). In FC, CK was positive all cases, the proportion of positive NH events was 92.2% (44.7-99.1). 4/5 cases were bright intensity (iMFI 7.0, 4.3-16.1) and one had low intensity (iMFI 3.18). (Fig. 9)

In IHC, VIM reaction was diffuse, strong (score 3) and observed in >75% on NH cells in almost all cases. Final IHC score was 11/12 (8-12). In FC, VIM was positive in all cases, the proportion of positive NH events was 89% (60.4-95.2), 4/5 had bright intensity (iMFI 7.0, 4.9-34), one had low intensity (iMFI 4.1). (Fig. 9)

In both IHC and FC desmin was negative in all cases. In IHC, few (<10%) scattered cells with diffuse strong reaction were present in all cases. Similarly, in FC rare DES positive events (7.3%, range 2.3-18.8) were observed among NH cells.

Patterns

For each antibody, the observed patterns in FC and IHC are presented in table 12 listing the absolute and relative numbers of cell type. According to data collected in this study, the expected patterns of each NH cell subgroup and the interpretation keys for CK, VIM and DES in FC compared to IHC are presented in table 13.

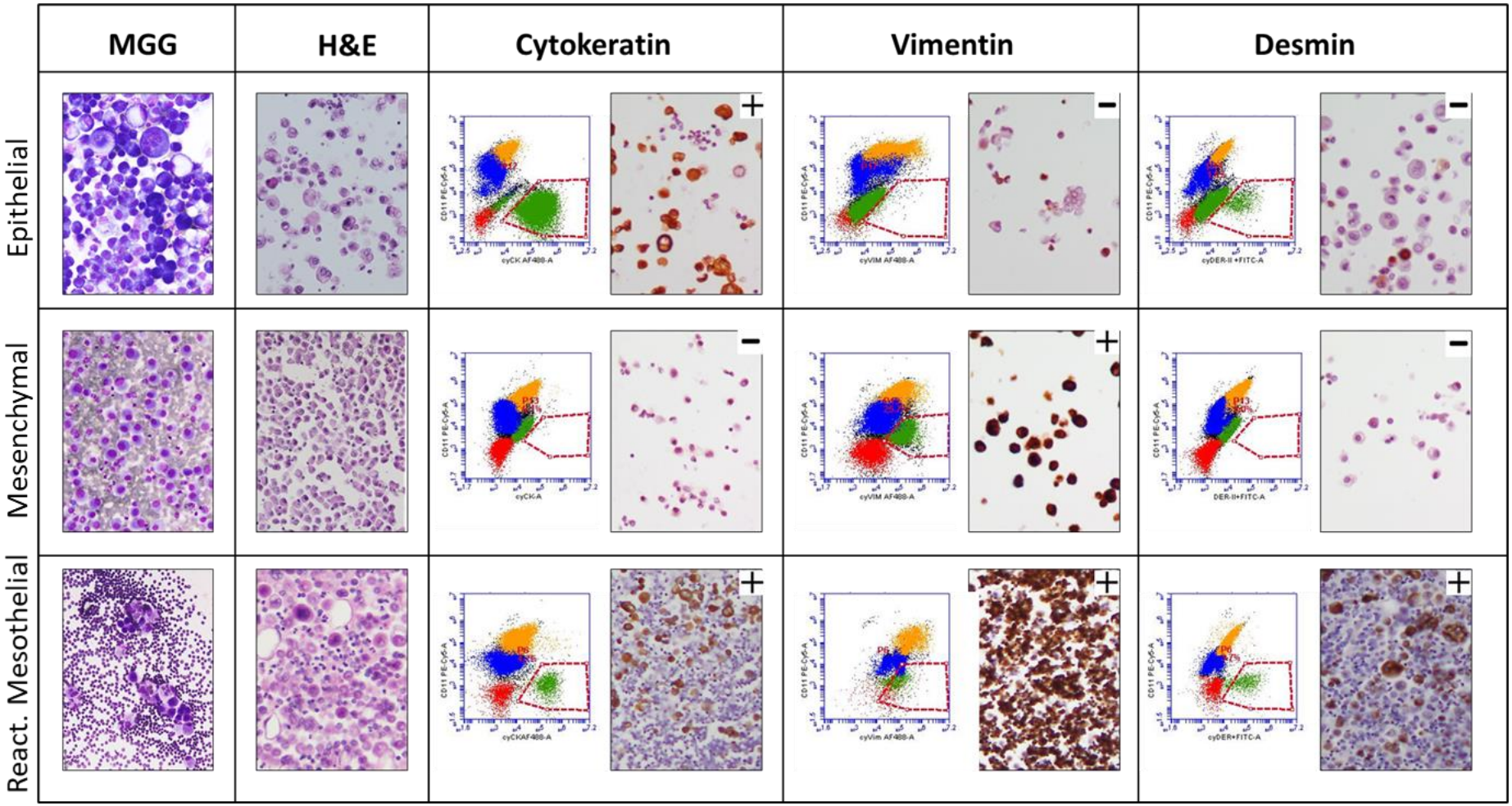

Figure 8. Exemplificative patterns of epithelial, mesenchymal, and reactive mesothelial cells in canine effusions. Epithelial: pleural effusion, lung adenocarcinoma. Mesenchymal: pleural effusion, rib osteosarcoma. Reactive mesothelial cells: pericardial effusion, rupture of cavitated right auricular mass. From left to right, cytospin preparation May-Grunwald Giemsa, cell block Haematoxylin and Eosin, flow cytometry scatter [CD11b PE-Cy5 /cytokeratin AF488 (CK AE1/AE3), CD11b PE-Cy5 /vimentin AF488 (V9), CD11b PE-Cy5 /desmin (DER-II) with FITC conjugated secondary antibody], and cell block immunohistochemistry [cytokeratin (CK AE1/AE3), vimentin (V9), desmin (DER-II); diaminobenzidine chromogen, Haematoxylin counterstained]

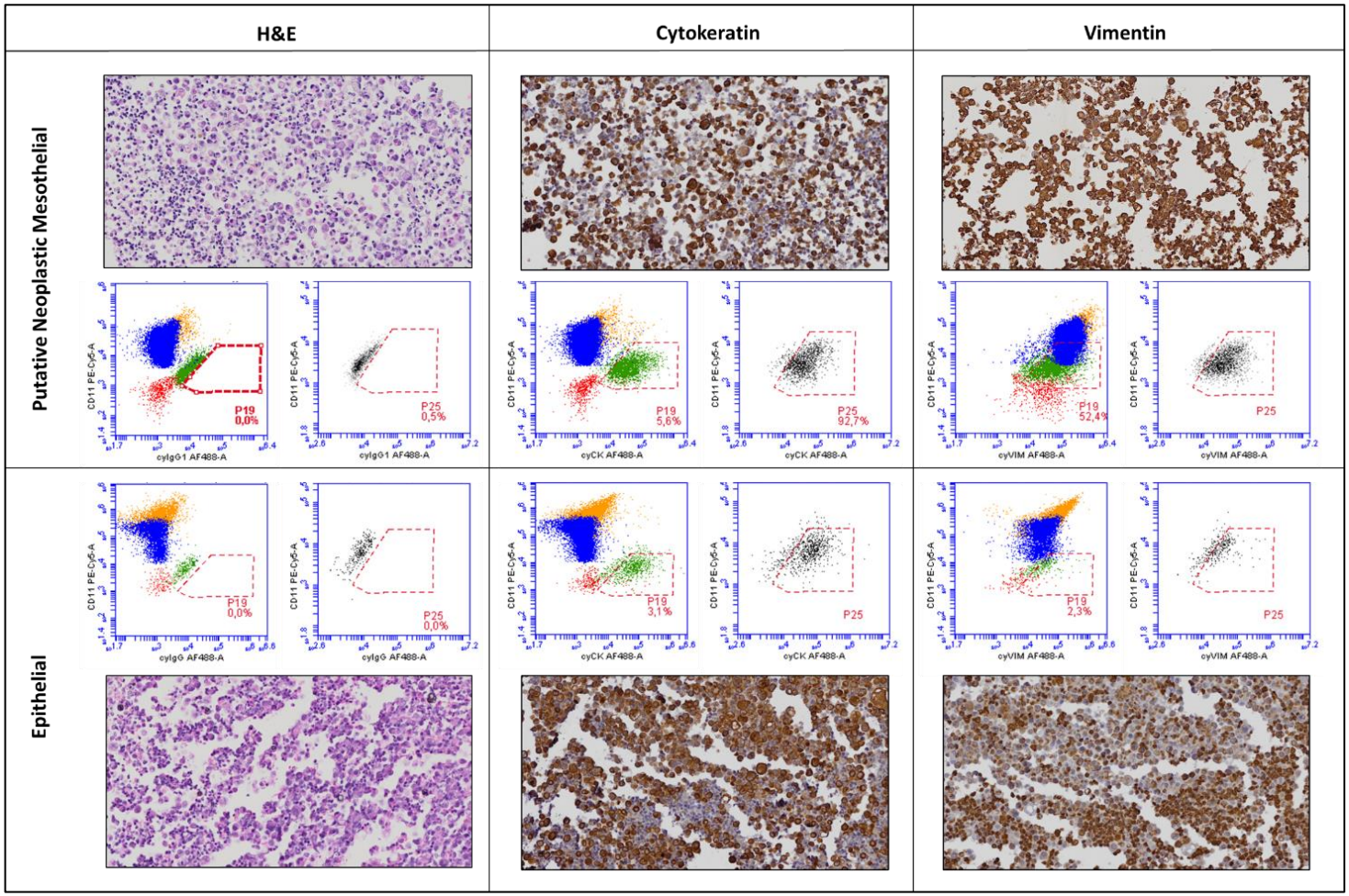

Figure 9. Immunohistochemistry and flow cytometry of putative neoplastic mesothelial cells and epithelial cells in canine effusions.

Immunohistochemistry on cell blocks, from left to right, H&E, cytokeratin (CK AE1/AE3), and vimentin (V9), diaminobenzidine chromogen, Haematoxylin counterstained. Flow cytometry dot plots (over all intact cells) and density plots (over large CD11b- events), from left to right, CD11b PE-Cy5/isotype (IgG AF488), CD11b PE-Cy5/cytokeratin AF488 (CK AE1/AE3), CD11b PE-Cy5/vimentin AF488 (V9).

Putative Neoplastic Mesothelial Cells: in immunohistochemistry, cytokeratin and vimentin are expressed with strong intensity and diffuse pattern in more than 75% of the cells. In flow cytometry, 92,7% and 91.1% of large CD11b- events are positive for cytokeratin and vimentin, respectively.

Epithelial Cells: in immunohistochemistry, cytokeratin is expressed with strong intensity and diffuse pattern in more than 75% of the cells, vimentin is expressed with moderate to strong intensity with patchy distribution within the cell in 50-75% of the cells. In flow cytometry, 86.2% of large CD11b- events are positive for cytokeratin, 51.2% of large CD11b- events are positive for vimentin with low intensity.

Table 12. Cytokeratin, vimentin, and desmin patterns in flow cytometry and immunohistochemistry on cell blocks in 24 canine effusions.

Flow Cytometry	Immunohistochemistry on cell block				Frequencies of patterns			
Interpretation	**Interpretation**	**Intensity**	**Pattern**	**Positive cells**	**Epithelial N=7**	**RM N=11**	**Putative MM N=5**	**Mesenchymal N=1**
Cytokeratin								
Positive bright	Positive	Strong	Diffuse	Almost all cell	6 (86%)	11 (100%)	4 (80%)	-
Positive low	Positive	Strong	Diffuse	Almost all cell	1 (14%)	-	1 (20%)	-
Negative	Negative	-	-	-	-	-	-	1 (100%)
Vimentin								
Positive bright	Positive	Strong	Diffuse	Almost all cell	-	5 (45%)	4 (80%)	1 (100%)
Positive low	Positive	Strong	Diffuse	Almost all cell	-	3 (27%)	1 (20%)	-
Positive low	Positive	Mod/Strong	Non-diffuse	Partial	3 (43%)	1 (9%)	-	-
Negative	Positive	Mod/Strong	Non-diffuse	Partial	3 (43%)	2 (18%)	-	-
Negative	Negative	-	-	-	1 (14%)	-	-	-
Desmin								
Positive bright	Positive	Strong	Diffuse	Almost all cell		8 (72%)		
Positive bright	Positive	Mod/Strong	Non-diffuse	Partial		1 (9%)		
Positive low	Positive	Mod/Strong	Non-diffuse	Partial		2 (18%)		
Negative	Negative	-	-	-	7 (100%)		5 (100%)	1 (100%)

RM, Reactive Mesothelial. MM, Mesothelioma.

Table 13. Frequent CK, VIM and DES patterns of epithelial, mesenchymal, reactive mesothelial and putative neoplastic mesothelial in canine effusions by in flow cytometry and immunohistochemistry on cell blocks.

	Flow Cytometry			**Immunohistochemistry on Cell Blocks**		
	Cytokeratin	**Vimentin**	**Desmin**	**Cytokeratin**	**Vimentin**	**Desmin**
Epithelial	Positive bright, high %.	Positive low, low %, or negative.	Negative (*).	Positive strong, diffuse, almost all cells.	Positive moderate/strong, patchy, low to moderate % of cells, or negative.	Negative (*).
Reactive Mesothelial	Positive bright, high %.	Variable (mainly positive).	Positive bright, moderate to high %.	Positive strong, diffuse, almost all cells.	Variable (mainly positive).	Positive (mostly strong, diffuse, in almost all cells).
Putative Neoplastic Mesothelial	Positive bright, high %.	Positive bright, high %.	Negative (*).	Positive strong, diffuse, almost all cells.	Positive strong, diffuse, almost all cells.	Negative (*).
Mesenchymal	Negative (*).	Positive bright, high %	Negative (*).	Negative (*).	Positive strong, diffuse, almost all cells.	Negative (*).

(*), rare to small numbers of positive events/cells consistent with reactive mesothelial cells can be seen.

3.4. DISCUSSION AND CONCLUSION

Flow cytometry has been increasingly used in the last years for hematopoietic cell immunophenotyping. On the other side, the phenotype of non-hematopoietic cells in cavitary effusions has been investigated through immunocytochemistry on smears (Przeździecki 2014, Hoingoous 2008, Raskin 2015) or, more recently, with immunohistochemistry on cell blocks (Zanoni 2012, Wallace 2015, Marcos 2017).

Non-hematopoietic cells in effusions comprise mostly reactive mesothelial cells and neoplastic cells deriving from both primary and metastatic tumours. The presence and the number of neoplastic cells in the fluid depend on the extension of the involved area and the tendency to exfoliate of the neoplasm. Epithelial and mesothelial tumours shed cells more readily than mesenchymal tumours. Further, reactive mesothelial cells are easily released in the effusion fluid in presence of any kind of injury or stimuli (Mustaers 2007).

Epithelial, reactive, and neoplastic mesothelial cell often have overlapping morphological features. Further, in effusions all cells acquire a round shape due to the surface tension and cells at different activation and degeneration stages are contemporary present (Raskin 2015). For these reasons, ancillary methods for immunophenotyping are often required.

In this study, flow cytometry has been applied for the first time to non-hematopoietic cells in effusions. Features of non-hematopoietic cells were described along with the adopted staining procedure and identification strategy. Further, three markers were used to characterise these cells and the results were compared with the immunohistochemical staining on cell blocks. Based on the results of this study, preliminary interpretation keys of a three-antibody panel for non-haematopoietic cells in effusion were suggested.

About non-hematopoietic cells identification

Effusion samples comprise a mixed population of inflammatory cells both hemopoietic (lymphocytes, neutrophils, and macrophages) and non-hemopoietic (reactive mesothelial cells). In case of neoplastic exfoliative disorders, a "third population" composed by cancer cells can be variably observed. The high variability in morphological presentation of neoplastic cells, particularly the non-hematopoietic ones, reflects the high variability FSC and SSC observed in flow cytometry.

As effusions display such variable populations in terms of cell types and morphology, the gating strategy is oriented to include the vast majority of the events, only cell debris are excluded. Doublets gate is used to prevent the inclusion in the analysis of clustered cells which would affect the FSC, SSC, and fluorescence features. Non-hematopoietic cells, especially the neoplastic ones, are often seen in clusters. Thus, the exclusion of doublets slightly affected the relative count, lowering it. However, this did not affect the final interpretation and it was likely due to the consistent presence of both

arrangements in every sample. This was also confirmed in immunohistochemistry on cell blocks, where, in all cases with cohesive clusters, single cells with identical staining features were also present. In a pilot study, different enzymatic solutions were investigated with the aim of dissociate these clusters and increase the yield of target cells. Different enzymatic (trypsin, hyaluronidase, collagenase, and accutase) and non-enzymatic (EDTA at high concentration) dissociation protocols were tested. Those protocols failed to provide a significant increase of single non-hematopoietic cells without severely affecting count of other populations or samples quality (large amounts of debris were seen). Further, dissociating enzymes may alter the antigen conformation, and prevent the binding with the antibody. Enzymatic dissociation should be further investigated, with particular interest in defining a rapid and effective protocol able to maintain the integrity of all cell and increase the yield of the target population. However, if cohesive clusters predominates and are the main cytological feature, the use of a different ancillary technique would be recommended, notably the immunohistochemistry on cell blocks.

Morphological scatters easily allowed the identification of lymphocytes and granulocytes. On the other side, non-hematopoietic cells, and monocytes/macrophages where more frequently undistinguishable, although a slight tendency to a higher SSC was observed in the latter population. Both non-hematopoietic and monocytes/macrophages had a higher autofluorescence than lymphocytes and granulocytes, this finding was more prominent in presence of high cytoplasmic foaminess, cellular debris, and RBC breakdown products in the RBC. This was likely due to the larger size of the cells, and to the presence of phagocytized material altering the fluorescence properties.

Non-hematopoietic cells were identified as CD44+ events which were negative to all other hematopoietic markers, and particularly to CD45. CD45 was used in pilot cases as identification marker for the intracytoplasmic staining, however it had poor and unpredictable performances: reduced intensity after fixation (especially in neutrophils) and often induced neutrophils to aggregate. CD45 negative events were consistently large and CD11b-, further CD11b clearly isolated lymphocytes and granulocytes. Combining the immunoreactivity of CD11b and the FSC, all four populations were easily detectable. The usefulness of CD11b as a good identification marker was further confirmed by magnetic cell sorting. Also, in pilot cases and in all included cases, all CD45 negative events were large and CD11b negative (and vice versa) confirming the consistency of this marker. Thus, CD11b was selected as identification marker because allowed the identification of all main populations in effusions. CD11b staining was run with a PE-Cy5 conjugated antibody, a stable signal intensity was observed after cytoplasmic staining and among cases, additionally the use of a PE-Cy5 conjugated antibody allowed to prepare a multicolour panel with more commonly available fluorochromes. Although in this series of cases, the only large CD11b negative events were the target population, the use of a screening panel including at least CD44, CD45 and CD11b remain mandatory. This is to ensure that all the putative non-hematopoietic cells (CD44+CD45-) are CD11b- and that all large CD11b- events are CD44+CD45-

. Further, it would allow to address the presence of possible confounding populations, for instances, some subsets of large CD11b- histiocytes in both their reactive and neoplastic form (Yamazaki 2014).

About non-hematopoietic cells immunoprofiles

Cells' characterisation includes the use of major lineage markers to distinguish hematopoietic from non-hematopoietic cells and among the latter epithelial from mesenchymal cells. In this vein, CD45, CK, and VIM are the first step markers in lineage characterisation (Raskin 2015). Additionally, in effusion, the presence of mesothelial cells should be considered, and CK/VIM coexpression suggest a mesothelial origin both in human and animals (King 2006, La Rocca 1984, Moroni 2006). This panel is already known to have limitations and exception but remain the first step for non-hematopoietic cell characterisation. In general, based on the literature the expected profiles using this panel are CD45-/CK+/VIM- for epithelial cells, CD45-/CK-/VIM+ for mesenchymal cells, CD45-/CK+/VIM+ for mesothelial cells. To further differentiate between reactive and neoplastic mesothelial cells DES was added to the panel. In human medicine this marker is specific for reactive mesothelial cells (Gill 2000, Davidson 2001, Hasteh 2010), while in veterinary sciences it has been reported also in their malignant counterpart (Hoingaus 2008, Przezdziecki 2014).

In epithelial cells CK expression was strong and its interpretation straightforward. CK was determined using a cocktail of two monoclonal antibodies (CK AE1/AE3) which recognize both low and high molecular weight cytokeratins (1-8, 10-16, 19). Most epithelial cells express more than one type of keratin, and the use of a cocktail ensures a positive reaction if at least one CK type is present. Further, CK profile is tissue/organ specific and the profile is often maintained or selectively changed during metastasis (i.e. CK7/CK20 profile in human breast and colorectal cancer). Thus, CK profile could help in the identification of the origin of metastatic disease. Further studies to investigate the CK profile of epithelial cells in effusions and primary tumour are warranted.

The evaluation of CK and VIM revealed and unexpected profile in both flow cytometry and immunohistochemistry. CK and VIM were frequently coexpressed in neoplastic epithelial cells supporting previous reports on effusion samples in immunocytochemistry (Przezdziecki 2014), immunohistochemistry on cell blocks (Marcos 2019) and tissues (Burgess 2009). Conversely, Wallace in 2015 did not report any reactivity to VIM in epithelial cells. VIM had a patchy or mixed staining pattern in a small to moderate proportion of cells (Fig. 9). The non expected positivity to VIM in epithelial cells may be due to an aberrant expression of this intermediate filament in some epithelial tumours. This has been demonstrated in canine lung (Burgess 2009) and mammary carcinomas (Raposo-Ferreira 2018). In particular, the uneven staining pattern also support the hypothesis that these cells undergo to type 3 epithelial-to-mesenchymal transition (EMT). IN EMT, epithelial cells downregulate the expression of adhesion proteins, and acquire a mesenchymal phenotype; they lose cell-cell and cell-matrix contact and gaining mobility facilitating the metastasis cascade (intravasation,

transport, extravasation and colonization) (Kalluri 2009). EMT is a complex mechanism, extensive phenotypical profiling could contribute to better understand their pathophysiology and profiling of epithelial cells in effusions could give an insight on phenotypical changes during metastasis and cellular adaptation. Alternatively, the acquired expression of VIM could be and adaptive change of these cells to the effusion environment.

CK and VIM coexpression was also a consistent feature of reactive mesothelial cells. However, in 30% of the cases there was only a moderate (25-50%) proportion of VIM positive cells. These cases showed an overlapping profile with epithelial cells. However, it should be noted that epithelial cells had a non-diffuse VIM pattern (patchy o mixed), whereas reactive mesothelial cells stained with a moderate to strong intensity and diffuse pattern. This different cytoplasmic distribution may reflect the ontogenic difference between acquired vimentin expression (epithelial) and innate expression (mesothelial). A similar strong and diffuse pattern was observed in the only case of mesenchymal cells and in putative neoplastic mesothelial cells. These findings further support the hypothesis that the patchy and uneven distribution of VIM in epithelial cells represent an acquired expression of this intermediate filament as opposed to the strong and diffuse expression in mesothelial and mesenchymal cells.

Both reactive and putative neoplastic mesothelial cells consistently coexpressed CK and VIM, similar findings were reported in effusions (Wallace 2015, Przezdziecki 2014, Hoingaus 2008) and tissues (Milne 2017, Geninet 2003, Morini 2006, , Reggeti 2005, Sato 2005, Vascellari 2011, D'angelo 2014). Negative reaction to vimentin has been also reported in reactive mesothelial cells (Tickman 1990, Marcos 2019). Although, this is in contrast with the findings in this case series, nearly one third of the cases showed a lower proportion of positive cells. It is possible that low to undetectable levels of vimentin in mesothelial cells can occur both related to their status of activation and neoplastic change.

Although CK/VIM profile provides useful information contributes to mesothelial cells identification, the mere definition of positivity and negativity do not ensure enough accuracy in diagnostic setting to distinguish between epithelial and mesothelial cells.

CK and VIM expression profile including the evaluation of the proportion of positive cells and the staining pattern may facilitate the differentiation between epithelial and mesothelial cells. However, the accuracy of this pattern alone is questionable and still does not allow the differentiation between reactive and neoplastic mesothelial.

For this reason, the use of additional mesothelial markers is recommended. HBME-1 and calretinin has been demonstrated as inconsistent in veterinary medicine (Caswell 2016). In humane medicine, WT1 is often used to discriminate mesothelial from epithelial cells with higher performances in identifying reactive mesothelial cells (Husain 2013). Recently, this marker has been used in canine and feline effusions showing promising results (100% sensitivity and specificity in mesothelial cell identification)

(Marcos 2019). Other markers have also been evaluated in immunohistochemistry on pericardial tissue (glucose transporter 1 and insulin-like growth factor II mRNA-binding protein 3) (Milne 2017). Desmin has been marginally used for this purpose in veterinary medicine. Its expression seems specific for mesothelial origin but not able to distinguish between reactive and neoplastic cells in effusion (Hoingaus 2008, Przezdziecki 2014), while it stained inconsistently mesothelial cells in pericardial tissue (Milne 2017). In this study, reactive mesothelial cells stained consistently and strongly for desmin in immunohistochemistry with a diffuse (70%) or focal (30%) cytoplasmic pattern. Additionally, putative neoplastic mesothelial cells were negative in all cases and rare scattered positive cells were observed in all neoplastic cases probably representing the associated reactive mesothelial cells component. These findings are in contrast with veterinary literature in dogs but support part of the studies in humans (Gill 2000, Davidson 2001, Hasteh 2010). Based on available data it is possible to hypothesized that desmin is variable expressed in mesothelial cells probably related to their activation and proliferation status and malignancy. Desmin loss can be related to a sort of undifferentiated phenotype of neoplastic mesothelial cells as known in muscular tumours (Evans 1983). The origin of desmin expression in mesothelial cells remain unknown and there is poor evidence of the intermediate filament profiles during embryologic development, reactive and neoplastic changes of mesothelial cells. Previous literature, in humane medicine, show variable and contrasting results; the use of different revealing methods, matrices, clones, and protocols does not allow a definitive indication about the usefulness of this marker. Methods specific for veterinary samples should be investigated including particularly antibodies cross reactivity, and staining protocols.

From the diagnostic point of view, the introduction of DES in combination with CK and VIM is strongly recommended to characterise non-haematopoietic cells in effusions. According to the presented results, a positive reaction is highly supportive of benign mesothelial origin, a negative result (with rare scattered positive cells) is expected in epithelial, mesenchymal (non-muscular), and neoplastic mesothelial (putative) cells.

About flow cytometry immunophenotyping

The immunophenotype of non-haematopoietic cells was concordant in flow cytometry and immunohistochemistry in 80% of the cases. In all discordant cases flow cytometry did not revealed a positive reaction for VIM in epithelial and reactive mesothelial cells. A false negative result could be due to absent signal (unstable binding, antigen loss or masking, lack of antigen saturation) or signal below the sensitivity of the instrument. Unstable binding and antigen loss were unlikely in these cases, indeed other cells in the same sample (hematopoietic cells) and non-hematopoietic cells in other samples were correctly stained using the same products and protocol. Lack of antigen saturation is related to stoichiometric impediment in the binding (as above, unlikely), or for improper titration. VIM titration

was performed on expected positive cells with low intensity (lymphocytes) in order to ensure a proper detection of low signals and verified in pilot cases.

Flow cytometric immunolabelling was studied in terms of subjective brightness and proportion of positive events, and compared with the immunohistochemical staining intensity, proportion of positive cells, and pattern. Interestingly, low intensity signals in flow cytometry were more frequently founded in samples with a non-diffused distribution (for all the three markers) than in samples with a non-strong intensity. In flow cytometry, signal brightness is related to the total amount of antigen in each cell, this is in contrast with IHC were staining intensity and the cytoplasmic pattern are independent parameters. For example, a cell with a large amount of antigen evenly distributed within the cytoplasm will have a high intensity score (strong) and diffuse cytoplasmic pattern in immunohistochemistry and a bright intensity in flow cytometry. Whereas, if a lower amount of antigen is condensed in a small area of the cytoplasm, this will have a high intensity score (strong) and a focal distribution in immunohistochemistry but a low intensity in flow cytometry (the amount of antigen-fluorochrome is lower than the previous example). In all false negative cases there was a lower proportion of positive cells which had moderate staining intensity or a patchy cytoplasmic pattern in immunohistochemistry. Additionally, haematopoietic populations express VIM, this could have induced an antigen-antibody competition making a weak signal difficult to detect. It is possible that in particular cases where more than one of these conditions are simultaneously present, the amount of binding antibody is insufficient for a clear detection leading to a false negative result in flow cytometry.

On the other side, a bright signal in flow cytometry was frequently found in samples with a strong diffuse expression in immunohistochemistry. This phenomenon was more commonly observed for CK, DES, and limited to putative neoplastic mesothelial and mesenchymal cells for VIM.

Therefore, in terms of diagnostic interpretation, a bright signal is consistent with a strong diffuse expression in immunohistochemistry, while a low signal is consistent with a focal/patchy/non-diffuse distribution in immunohistochemistry. A negative result in flow cytometry should be interpreted as true negative. However, some VIM-negative results could represent an underestimation of an IHC-positive focal/patchy/non-diffuse signal in epithelial (40%) and reactive mesothelial cells (20%).

To sum up, flow cytometry can be used to characterise non-hematopoietic cells in effusions providing the same results of immunohistochemistry on cells blocks for CK and DES, while VIM expression may be underestimated.

Considering the relative high variability in the expression of single markers, when characterising non-hematopoietic cells, the value of the whole panel has probably more value than the interpretation of each single marker. Therefore, based on the results obtained in this study, once the non-hematopoietic nature of the cells is confirmed (CD45-), CK should be the first lineage marker to be considered because

it allows to rule out mesenchymal cells. Then, DES allows to identify reactive mesothelial cells and finally, VIM is expected to be positive bright in neoplastic mesothelial cells and negative or positive low in epithelial cells (Fig. 10). A similar diagnostic algorithm can be applied for the interpretation of the same markers in immunohistochemistry on cell blocks (Fig. 11).

Although the results were straightforward for some aspects, the diagnostic value of this approach should be prospectively validated on a larger series of cases. Another limitation is the lack of a definitive histological diagnosis in most of the cases. In particular, although collateral data were highly supportive of neoplastic mesothelial origin, carcinomatosis or severe mesothelial hyperplasia of unknown origin could not be fully ruled out. This possibly affected the results of this approach, and these results should be further confirmed in cases with a definitive histological diagnosis. Further, all these cases showed consist and strong coexpression in IHC on cell blocks of CK and VIM.

Also, the multicolour characterisation and study of signals intensity and markers coexpression would be beneficial to further investigate non-haematopoietic cells in effusions. A two-colour approach has recently been demonstrated a useful tool in immunocytochemistry (Moore 2015, Sawa 2018). Flow cytometry provides major advantages in those aspects, and further investigations in this direction are recommended.

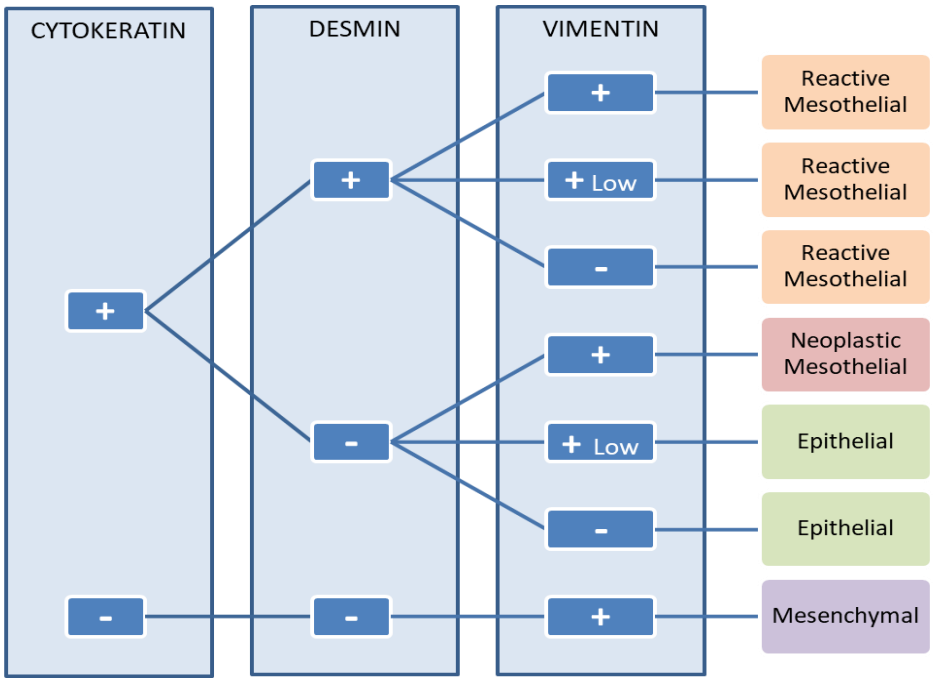

Figure 10. Diagnostic algorithm for non-hematopoietic profile interpretation in flow cytometry of effusions. The panel should be applied once confirmed the non-hematopoietic origin.

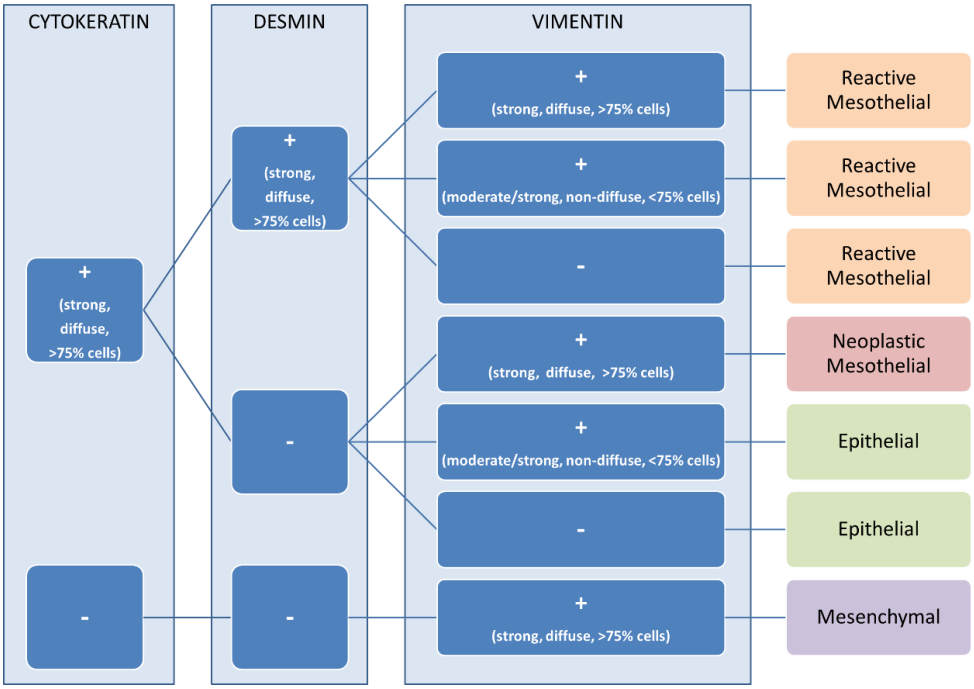

Figure 11. Diagnostic algorithm for non-hematopoietic profile interpretation in immunohistochemistry on cell blocks of effusions. The panel should be applied once confirmed the non-hematopoietic origin or together with hematopoietic markers

FINAL CONSIDERATIONS

This study investigated three methods that can improve the diagnostic yield of effusion analysis by extending the potential of ancillary testing and refining the cytological diagnosis.

Both the tested cell block methods are reliable preparations for immunohistochemical studies. Observed differences can be useful in particular subsets of samples (i.e., cell tube block in haemorrhagic, poorly cellular, or samples with low volumes available). The methods should also be chosen depending on technical and management features of clinics/laboratories. Additionally, cell tube blocks can be prepared directly in the clinic reducing the turnaround time for processing the sample. Finally, the outstanding usefulness of cells blocks, is the possibility to apply immunohistochemical stainings with minimal optimization and the easy storing of cellular material. The latter could represent a costless opportunity for research or to run further test at a later time.

Although automated cell count of effusion is routinely performed in most of the laboratories, only total counts are considered for diagnostic purposes. Apart from red blood cells and nucleated cell counts, cytograms can provide additional information without adding costs to the analysis. The high specificity of ADVIA 120 cytogram interpretation reasonably predicts certain cytological outcomes, this can allow a faster and selected cytological examination and can speed up the decisional process for additional tests.

A flow cytometric gating and staining strategy able to identify and characterise non-haematopoietic cells in effusions was provided. Overall, flow cytometry ensures similar results to immunohistochemistry on cell blocks. Staining for cytokeratin and desmin were straightforward, while the interpretation of vimentin should not be limited to the interpretation of at a positive/negative level. The different immunohistochemical patterns and flow cytometric intensity allow to differentiate epithelial from mesothelial cells in most of the cases. From the diagnostic point of view, a full panel interpretation through the described algorithm has a much higher value than the interpretation of single antibodies both in flow cytometry and immunohistochemistry. This strategy is also the forerunner for future validations of other antibodies specific for non-hematopoietic cells, with the primary goal to identify markers to differentiate neoplastic from reactive mesothelial cells; flow cytometric multicolour analysis is an additional value for this purpose.

In conclusion, all methods considered showed benefits and drawbacks, based on the results of this project and on the available literature, a working scheme for effusions analysis is provided (Fig.12). The scheme is aimed to suggest a possible workflow for the diagnostic management of effusion samples integrating the conventional standard analysis with more advanced ancillary techniques, considering

also the possibility to store material for further tests and research purposes. The integration of different ancillary methods should be further investigated to determine the performances of each single method and validate the integrated approach. This could reveal differences in performances between different subsets of cases and maximise the diagnostic potential for each patient.

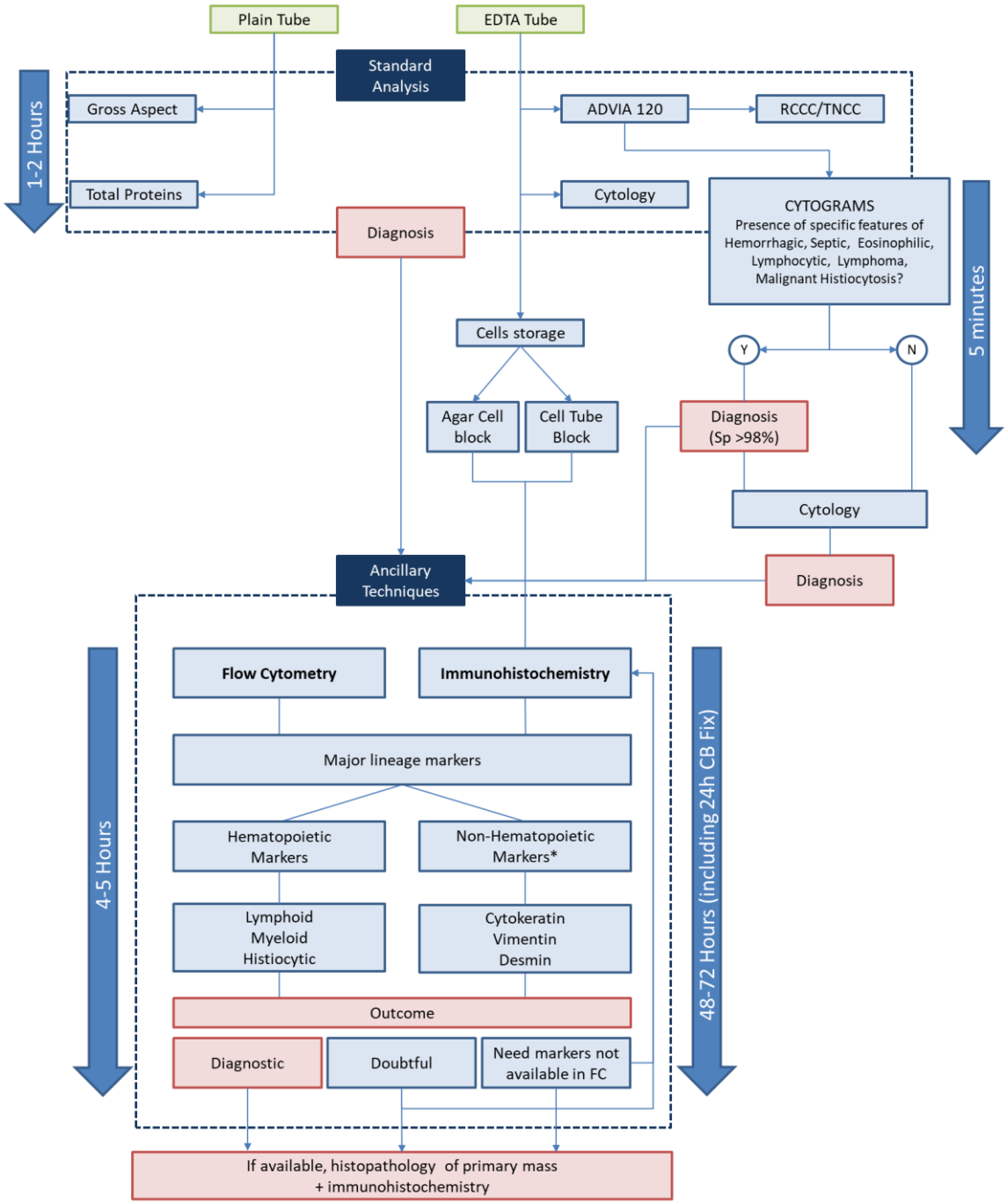

Figure 12. Diagnostic workflow for effusions analysis integrating standard analysis and ancillary tests. Approximate times for the analysis are reported. (*) Refer to Fig. 10 and Fig. 11 for diagnostic algorithm for markers interpretation in flow cytometry and immunohistochemistry.

REFERENCES

Addis B, Roche H. Problems in mesothelioma diagnosis. *Histopathology*. 2009 Jan;54(1):55-68.

Advani AS, Rodriguez C, Jin T, Jawde RA, Saber W, Baz R, Kalaycio M, Sobecks R, Sekeres M, Tripp B, Hsi E. Increased C-kit intensity is a poor prognostic factor for progression-free and overall survival in patients with newly diagnosed AML. *Leuk Res*. 2008 Jun;32(6):913-8.

Afify AM, Al-Khafaji BM, Paulino AF, Davila RM. Diagnostic use of muscle markers in the cytologic evaluation of serous fluids. *Appl Immunohistochem Mol Morphol*. 2002 Jun;10(2):178-82.

Aulesa C, Mainar I, Prieto M, Cobos N, Galimany R. Use of the ADVIA 120 hematology analyser in the differential cytologic analysis of biological fluids (cerebrospinal, peritoneal, pleural, pericardial, synovial, and others). *Lab Hematol*. 2003;9:214–224.

Baker, R. & Lumsden, J. H. (2000) Pleural and peritoneal fluids. In: *Color Atlas of Cytology of the Dog and Cat*. 1st edn., eds. R. Baker and J.H. Lumsden. Mosby, MO, USA. p164

Bauer N, Moritz A. Flow cytometric analysis of effusions in dogs and cats with the automated hematology analyser ADVIA 120. *Vet Rec*. 2005;156:674–678.

Bertazzolo W, Bonfanti U, Mazzotti S, Gelain ME. Cytologic features and diagnostic accuracy of analysis of effusions for detection of ovarian carcinoma in dogs. *Vet Clin Pathol*. 2012 Mar;41(1) pp.127-132.

Bird SD. Mesothelial primary cilia of peritoneal and other serosal surfaces. *Cell Biol Int* 2004; 28:151–9.

Bohn AA. Analysis of Canine Peritoneal Fluid Analysis. *Vet Clin N Am-Small* 2017; 47(1):123-133.

Bolen JW, Hammar SP, McNutt MA. Reactive and neoplastic serosal tissue. A light-microscopic, ultrastructural, and immunocytochemical study. *Am J Surg Pathol*. 1986 Jan;10(1):34-47.

Brisson BA, Reggeti F, Bienzle D. Portal site metastasis of invasive mesothelioma after diagnostic thoracoscopy in a dog. *J Am Vet Med Assoc*. 2006 Sep 15;229(6):980-3.

Brudvig JM, Swenson CL. Total nucleated cell and leukocyte differential counts in canine pleural and peritoneal fluid and equine synovial fluid samples: comparison of automated and manual methods. *Vet Clin Pathol*. 2015 Dec;44(4):570-9.

Burgess HJ, Kerr ME. Cytokeratin and vimentin co-expression in 21 canine primary pulmonary epithelial neoplasms. *J Vet Diagn Invest*. 2009;21:815-820.

Caswell JF, Williams KJ. Respiratory system. In *Maxie MG, eds. Jubb, Kennedy and Palmer's pathology of domestic animals*. 6th ed. St. Louis, MO: Elsevier; 2016).

Comazzi S, Gelain ME. Use of flow cytometric immunophenotyping to refine the cytological diagnosis of canine lymphoma. *Vet J*. 2011 May;188(2):149-55.

Cowell RL, Valenciano AC. *Diagnostic cytology and hematology of the dog and cat*. Fourth edition, 2014.

Crapanzano JP, Heymann JJ, Monaco S, Nassar A, Saqi A. The state of cell block variation and satisfaction in the era of molecular diagnostics and personalized medicine. *Cytojournal*. 2014;11:7.

Dabbs DJ: Immunohistology of metastatic carcinoma of unknown primary. In Dabbs DJ (ed): *Diagnostic immunohistochemistry*, ed 2, New York, 2006, Churchill Livingstone.

D'Angelo AR, Di Francesco G. Sclerosing peritoneal mesothelioma in a dog: histopathological, histochemical and immunohistochemical investigations. *Vet Ital*. 2014 Dec 29;50(4):301-5.

Davidson B, Nielsen S, Christensen J, Asschenfeldt P, Berner A, Risberg B, Johansen P. The Role of Desmin and N-Cadherin in Effusion Cytology A Comparative Study Using Established Markers of Mesothelial and Epithelial Cells. *Am J Surg Pathol*. 2001;25, 1405–1412.

Davidson B. Malignant Effusions: From Diagnosis to Biology. *Diagn Cytopathol*. 2004; 31, 246-252.

Davidson B. Malignant Non hematological Effusion Characterisation by Flow Cytometry. *Acta Cytol*. 2016;60(4):365-371.

Dempsey SM, Ewing PJ. A Review of the Pathophysiology, Classification, and Analysis of Canine and Feline Cavitary Effusions. *J Am Anim Hosp Assoc*. 2011;47:1-11.

Di Paolo N, Sacchi G, De Mia M, Gaggiotti E, Capotondo L, Rossi P, et al. Morphology of the peritoneal membrane during continuous ambulatory peritoneal dialysis. *Nephron* 1986; 44:204–11.

Dongre A, Weinberg RA. New insights into the mechanisms of epithelial-mesenchymal transition and implications for cancer. *Nat Rev Mol Cell Biol*. 2019 Feb;20(2):69-84.

Duque C, Parent J, Bienzle D. The immunophenotype of blood and cerebrospinal fluid mononuclear cells in dogs. *J Vet Intern Med*. 2002 Nov-Dec;16(6):714-9.

Fernandes NCCA, Guerra JM, Réssio RA, et al. Liquid-based cytology and cell block immunocytochemistry in veterinary medicine: comparison with standard cytology for the evaluation of canine lymphoid samples. *Vet Comp Oncol*. 2016;14:107-116.

Ferrandez-Izquierdo A, Navarro-Fos S, Gonzalez-Devesa M, Gil-Benso R, Llombart-Bosch A. Immunocytochemical typification of mesothelial cells in effusions: in vivo and in vitro models. *Diagn Cytopathol*. 1994;10(3):256-62.

Foley-Comer AJ, Herrick SE, Al-Mishlab T, Prêle CM, Laurent GJ, Mutsaers SE. Evidence for incorporation of free-floating mesothelial cells as a mechanism of serosal healing*. J Cell Sci*. 2002 Apr 1;115(Pt 7):1383-9.

Geisinger KR, Stanley MW, Raab S, Silverman J, Abati A. *Modern Cytopathology*. Philadelphia, PA: Churchill Livingston; 2004: pp. 257-280.

Gelain ME, Mazzilli M, Riondato F, Marconato L, Comazzi S. Aberrant phenotypes and quantitative antigen expression in different subtypes of canine lymphoma by flow cytometry. *Vet Immunol Immunopathol*. 2008 Feb 15;121(3-4):179-88.

Geninet C., Bernex F., Rakotovao F., Crespeau F.L., Parodi A.L. & Fontaine J.J. 2003. Sclerosing peritoneal mesothelioma in a dog - a case report. *J Vet Med A Physiol Pathol Clin Med*, 50(8), 402-405.

Gill SA, Meier PA, Kendall BS. Use of desmin immunohistochemistry to distinguish between mesothelial cells and carcinoma in serous fluid cell block preparations. *Acta Cytol*. 2000;44:976-980.

Gorman ME, Villarroel A, Tornquist SJ, Flachsbart J, Warden A, Boeder L. Comparison between manual and automated total nucleated cell counts using the ADVIA 120 for pleural and peritoneal fluid samples from dogs, cats, horses, and alpacas. *Vet Clin Pathol*. 2009;38:388– 391.

Grieco V, Patton V, Romussi S, Finazzi M. Cytokeratin and vimentin expression in normal and neoplastic canine prostate. *J Comp Pathol*. 2003 Jul;129(1):78-84.

Hasteh F, Lin GY, Weidner N, Michael CW. The use of immunohistochemistry to distinguish reactive mesothelial cells from malignant mesothelioma in cytologic effusions. *Cancer Cytopathol*. 2010 Apr 25;118(2):90-6.

Heinrich DA, Avery AC, Henson MS, et al. Cytology and the cell block method in diagnostic characterisation of canine lymphadenopathy and in the immunophenotyping of nodal lymphoma. *Vet Comp Oncol*. 2019;17:365-375.

Hirschberger J, DeNicola DB, Hermanns W, Kraft W. Sensitivity and specificity of cytologic evaluation in the diagnosis of neoplasia in body fluids from dogs and cats. *Vet Clin Pathol*. 1999;28, 142-146.

Höinghaus R, Hewicker-Trautwein M, Mischke R. Immunocytochemical differentiation of canine mesenchymal tumours in cytologic imprint preparations. *Vet Clin Pathol*. 2008;37, 104-11.

Husain AN, Colby T, Ordonez N, et al. Guidelines for pathologic diagnosis of malignant mesothelioma: 2012 update of the consensus statement from the International Mesothelioma Interest Group. *Arch Pathol Lab Med*. 2013;137:647-667.

Jain D, Mathur SR, Iyer VK. Cell blocks in cytopathology: A review of preparative methods, utility in diagnosis and role in ancillary studies. *Cytopathology*. 2014;25:356-371.

Jantz MA, Antony VB. Pathophysiology of the pleura. *Respiration*. 2008;75(2):121-33.

Kalluri R. EMT: when epithelial cells decide to become mesenchymal-like cells. *J Clin Invest*. 2009 Jun;119(6):1417-9.

King JE, Thatcher N, Pickering CA, Hasleton PS. Sensitivity and specificity of immunohistochemical markers used in the diagnosis of epithelioid mesothelioma: a detailed systematic analysis using published data. *Histopathology*. 2006 Feb;48(3):223-32.

LaRocca PJ, Rheinwald JG. Coexpression of simple epithelial keratins and vimentin by human mesothelium and mesothelioma in vivo and in culture. *Cancer Res*. 1984 Jul;44(7):2991-9.

Lin O. Challenges in the interpretation of peritoneal cytologic specimens. *Arch Pathol Lab Med*. 2009 May;133(5):739-42.

Machida, N., Tanaka, R., Takemura, N., et al. (2004) Development of pericardial mesothelioma in Golden retrievers with a long-term history of idiopathic haemorrhagic pericardial effusion. *J Comp Pathol* 131, 166-175

Maher I, Tennant KV, Papasouliotis K. Effect of storage time on automated cell count and cytological interpretation of body cavity effusions. *Vet Rec*. 2010 Oct 2;167(14):519-22.

Marcos R, Marrinhas C, Malhão F, Canadas A, Santos M, Caniatti M. The cell tube block technique and an immunohistochemistry panel including Wilms tumour 1 to assist in diagnosing cavitary effusions in dogs and cats. *Vet Clin Pathol*. 2019;48:50-60.

Marcos R, Santos M, Marrinhas C, Caniatti M, Marcos CR. Cell tube block: a new technique to produce cell blocks from fluid cytology samples. *Vet Clin Pathol*. 2017;46:195-201.

Martini V, Melega M, Riondato F, Marconato L, Cozzi M, Bernardi S, Comazzi S, Aresu L. A retrospective study of flow cytometric characterisation of suspected extranodal lymphomas in dogs. *J Vet Diagn Invest*. 2018 Nov;30(6):830-836.

Menezes RC, Madeira MF, Ferreira LC, Barbosa Filho CJL, Miranda LHM, Figueiredo FB. Cell-block Immunohistochemistry of Bone Marrow Aspirates: A Novel Tool to Improve the Diagnosis of Leishmania Infection in Dogs. *J Comp Pathol*. 2016;154:157-160.

Milne E, Martinez Pereira Y, Muir C, et al. Immunohistochemical differentiation of reactive from malignant mesothelium as a diagnostic aid in canine pericardial disease. *J Small Anim Pract*. 2018;59: 261-271.

Mohanty SK, Dey P. Serous effusions: diagnosis of malignancy beyond cytomorphology. An analytic review. *Postgrad Med J*. 2003 Oct;79(936):569-74.

Moore AR, Coffey E, Leavell SE, Krafsur G, Duncan C, Dowers K, Santangelo KS. Canine bicavitary carcinomatosis with transient needle tract metastasis diagnosed by multiplex immunocytochemistry. *Vet Clin Pathol*. 2016 Sep;45(3):495-500.

Morini M., Bettini G., Morandi F., Burdisso R. & Marcato P.S. 2006. Deciduoid peritoneal mesothelioma in a dog. *Vet Pathol*, 43(2), 198-201.

Mor-Vaknin N, Punturieri A, Sitwala K, Markovitz DM. Vimentin is secreted by activated macrophages. *Nat Cell Biol*. 2003; 5:59-63.

Mutsaers SE, Whitaker D, Papadimitriou JM. Mesothelial regeneration is not dependent on subserosal cells. *J Pathol*. 2000 Jan;190(1):86-92.

Mutsaers SE, Wilkosz S. Structure and function of mesothelial cells. *Cancer Treat Res*. 2007;134:1-19.

Mutsaers SE. The mesothelial cell. *Int J Biochem Cell Biol*. 2004 Jan;36(1):9-16.

Ordóñez NG. The diagnostic utility of immunohistochemistry and electron microscopy in distinguishing between peritoneal mesotheliomas and serous carcinomas: a comparative study. *Mod Pathol*. 2006 Jan;19(1):34- 48.

Ortolani C. *Citometria a flusso (Flow Cytometry)*. First Edition, Edi. Ermes, 2019

Pillai V, Dorfman DM. Flow Cytometry of Nonhematopoietic Neoplasms. *Acta Cytol*. 2016;60(4):336-343.

Pinto da Cunha N, Giordano A, Caniatti M, Paltrinieri S. Analytical validation of the Sysmex XT-2000iV for cell counts in canine and feline effusions and concordance with cytologic diagnosis. *Vet Clin Pathol*. 2009;38:230– 241.

Pires MA, Seixas F, Palmeira C, Payan-Carreira R. Histopathologic and immunohistochemical exam in one case of canine endometrial adenocarcinoma. *Reprod Domest Anim*. 2010 Jun;45(3):545-9.

Politi E, Kandaraki C, Apostolopoulou C, Kyritsi T, Koutselini H. Immunocytochemical Panel for Distinguishing Between Carcinoma and Reactive Mesothelial Cells in Body Cavity Fluids. *Diagn Cytopathol*. 2005; 32, 151-154.

Priest HL, Hume KR, Killick D, et al. The use, publication and future directions of immunocytochemistry in veterinary medicine: A consensus of the Oncology-Pathology Working Group. *Vet Comp Oncol*. 2017;15:868–880.

Przeździecki R, Sapierzyński R. Using of immunocytochemistry in differential diagnosis of neoplasms of serosal cavities in dogs. *Pol J Vet Sci*. 2014;17:149-159.

Ramos-Vara JA, Kiupel M, Baszler T, Bliven L, Brodersen B, Chelack B, Czub S, Del Piero F, Dial S, Ehrhart EJ, Graham T, Manning L, Paulsen D, Valli VE, West K; American Association of Veterinary Laboratory Diagnosticians Subcommittee on Standardization of Immunohistochemistry. Suggested guidelines for immunohistochemical techniques in veterinary diagnostic laboratories. *J Vet Diagn Invest*. 2008 Jul;20(4):393-413.

Raskin R, Meyer D. Canine and Feline Cytology, *A Color Atlas and Interpretation Guide*. 3nd Edition, Elselvier, 2015.

Raskin RE, Vickers J, Ward JG, Toland A, Torrance AG. Optimized immunocytochemistry using leukocyte and tissue markers on Romanowsky-stained slides from dogs and cats. *Vet Clin Pathol*. 2019 Oct;48 Suppl 1:88-97.

Raposo-Ferreira, T., Brisson, B. K., Durham, A. C., Laufer-Amorim, R., Kristiansen, V., Puré, E., Volk, S. W., & Sorenmo, K. Characteristics of the Epithelial-Mesenchymal Transition in Primary and Paired Metastatic Canine Mammary Carcinomas. *Vet Pathol*. 2018;55(5):622-633.

Reggeti F, Brisson B, Ruotsalo K, Southorn E, Bienzle D. Invasive epithelial mesothelioma in a dog. *Vet Pathol*. 2005; 42, 77-81.

Riccardi E, Grieco V, Verganti S, Finazzi M. Immunohistochemical diagnosis of canine ovarian epithelial and granulosa cell tumours. *J Vet Diagn Invest*. 2007 Jul;19(4):431-5.

Rolls GO, Farmer NJ, Hall JB. *Artifacts in the histological and cytological preparations*. Leica Microsystem Education System. Melbourne: Leica Microsystems; 2010;84–85.

Rout ED, Avery PR. Lymphoid Neoplasia: Correlations Between Morphology and Flow Cytometry. *Vet Clin N Am-Small*. 2017 Jan;47(1):53-70.

Saqi A. The State of Cell Blocks and Ancillary Testing Past, Present, and Future. *Arch Pathol Lab Med*. 2016;140:1318-1322.

Sato T., Miyoshi T., Shibuya H., Fujikura J., Koie H. & Miyazaki Y. 2005. Peritoneal biphasic mesothelioma in a dog. *J Vet Med A Physiol Pathol Clin Med*, 52(1), 22-25.

Sawa M, Inoue M, Yabuki A, et al. Rapid immunocytochemistry for the detection of cytokeratin and vimentin: assessment of its diagnostic value in neoplastic diseases of dogs. *Vet Clin Pathol*. 2017;46:172-178.

Sawa M, Yabuki A, Kohyama M, Miyoshi N, Yamato O. Rapid multiple immunofluorescent staining for the simultaneous detection of cytokeratin and vimentin in the cytology of canine tumours. *Vet Clin Pathol*. 2018 Jun;47(2):326-332.

Shapiro, H. M. (2003) *Practical Flow Cytometry*, 4th editon. Wiley-Liss, New York.

Shidham VB, Mary Falzon. Serous effusions. In: Gray W, Kocjan G, eds. *Diagnostic Cytopathology*, 3rd Edition. London: Elsevier. 2010: 115-175.

Stockham SL, Scott MA. *Foundamentals of veterinary clinical pathology*. Second edition, 2008.

Su XY, Li GD, Liu WP, Xie B, Jiang YH. Cytological differential diagnosis among adenocarcinoma, epithelial mesothelioma, and reactive mesothelial cells in serous effusions by immunocytochemistry. *Diagn Cytopathol*. 2011 Dec;39(12):900-8.

Taylor BE, Leibman NF, Luong R, Loar AS, Craft DM. Detection of carcinoma micrometastases in bone marrow of dogs and cats using conventional and cell block cytology. *Vet Clin Pathol*. 2013;42:85-91.

Tickman RJ, Cohen C, Varma VA, Fekete PS, DeRose PB. Distinction between carcinoma cells and mesothelial cells in serous effusions. Usefulness of immunohistochemistry. *Acta Cytol*. 1990;34:491-496.

Vascellari M, Carminato A, Camali G, Melchiotti E, Mutinelli F. Malignant mesothelioma of the tunica vaginalis testis in a dog: histological and immunohistochemical characterisation. *J Vet Diagn Invest*. 2011 Jan;23(1):135-9.

Villiers E, Baines S, Law AM, Mallows V. Identification of acute myeloid leukemia in dogs using flow cytometry with myeloperoxidase, MAC387, and a canine neutrophil-specific antibody. *Vet Clin Pathol*. 2006 Mar;35(1):55-71.

Wallace KA, Goldschmidt MH, Patel RT. Converting fluid-based cytologic specimens to histologic specimens for immunohistochemistry. *Vet Clin Pathol*. 2015;44:303-309.

Weiss DJ. Flow cytometric evaluation of hemophagocytic disorders in canine. *Vet Clin Pathol*. 2002;31(1):36-41.

Whitaker D, Papadimitrou J. Mesothelial healing: morphological and kinetic investigations. *J Pathol* 1985; 145:159–75.

Whitaker D. The cytology of malignant mesothelioma. *Cytopathology*. 2000 Jun;11(3):139-51.

Williams JD, Craig KJ, von Ruhland C, Topley N, Williams GT, for The Biopsy Registry Study Group. The natural course of peritoneal membrane biology during peritoneal dialysis. *Kidney Int* 2003; 64(Suppl 88):S43–9.

Yamazaki H, Takagi S, Oh N, Hoshino Y, Hosoya K, Okumura M. Comparative analysis of mRNA expression of surface antigens between histiocytic and nonhistiocytic sarcoma in dogs. *J Vet Intern Med*. 2014 Jan-Feb;28(1):204-10.

Yáñez-Mó M, Lara-Pezzi E, Selgas R, Ramírez-Huesca M, Domínguez-Jiménez C, Jiménez-Heffernan JA, Aguilera A, Sánchez-Tomero JA, Bajo MA, Alvarez V, Castro MA, del Peso G, Cirujeda A, Gamallo C, Sánchez-Madrid F, López-Cabrera M. Peritoneal dialysis and epithelial-to-mesenchymal transition of mesothelial cells. *N Engl J Med*. 2003 Jan 30;348(5):403-13.

Yao V, Platell C, Hall JC. Role of peritoneal mesothelial cells in peritonitis. *Br J Surg*. 2003 Oct;90(10):1187-94.

Yung S, Chan TM. Mesothelial cells. *Perit Dial Int*. 2007 Jun;27 Suppl 2:S110-5.

Zanoni DS, Grandi F, Rocha NS. Use of the agarose cell block technique in veterinary diagnostic cytopathology: an "old and forgotten" method. *Vet Clin Pathol*. 2012;41:307-308.